Raytheon

OCEAN CURRENT

VISIBLE/INFRARED IMAGER/RADIOMETER SUITE ALGORITHM THEORETICAL BASIS DOCUMENT

Version 4: May 2001

Caitlin P. Mullen

Dorlisa Hommel
William Emery, Science Team Member
University of Colorado

RAYTHEON SYSTEMS COMPANY
Information Technology and Scientific Services
4400 Forbes Boulevard
Lanham, MD 20706

SBRS Document #: Y2403

EDR: Ocean Currents

Doc No: Y2403
Version: 4
Revision: 0

	FUNCTION	NAME	SIGNATURE	DATE
PREPARED BY	EDR DEVELOPER	C. MULLEN		4/28/2000
APPROVED BY	RELEVANT LEAD	D. HOMMEL		
APPROVED BY	CHIEF SCIENTIST	S. MILLER		
RELEASED BY	ALGORITHM IPT LEAD	P. KEALY		

TABLE OF CONTENTS

Page

LIST OF FIGURES iii

LIST OF TABLES iv

GLOSSARY OF ACRONYMS v

ABSTRACT vii

1.0 INTRODUCTION 1
- 1.1 PURPOSE 1
- 1.2 SCOPE 1
- 1.3 VIIRS DOCUMENTS 1
- 1.4 REVISIONS 2

2.0 EXPERIMENT OVERVIEW 3
- 2.1 OBJECTIVES OF OCEAN CURRENT RETRIEVALS 3
- 2.2 INSTRUMENT CHARACTERISTICS 4
- 2.3 RETRIEVAL STRATEGY 4

3.0 ALGORITHM DESCRIPTION 5
- 3.1 PROCESSING OUTLINE 6
- 3.2 ALGORITHM INPUT 6
  - 3.2.1 VIIRS Data 6
  - 3.2.2 Non-VIIRS Data 7
- 3.3 THEORETICAL DESCRIPTION OF OCEAN CURRENT RETRIEVALS 7
  - 3.3.1 Physics of the Problem 7
  - 3.3.2 Mathematical Description of the Algorithm 18
  - 3.3.3 Archived Algorithm Output 20
  - 3.3.4 Variance and Uncertainty Estimates 20
- 3.4 ALGORITHM EVALUATION AND SENSITIVITY STUDIES 22
  - 3.4.1 Calibration Errors 32
  - 3.4.2 Instrument Noise 32
- 3.5 PRACTICAL CONSIDERATIONS 32
  - 3.5.1 Numerical Computation Considerations 32
  - 3.5.2 Programming and Procedural Considerations 32
  - 3.5.3 Configuration of Retrievals 32
  - 3.5.4 Quality Assessment and Diagnostics 32

3.5.5 Exception Handling 32
3.6 ALGORITHM VALIDATION 33
4.0 ASSUMPTIONS AND LIMITATIONS 37
4.1 ASSUMPTIONS 37
4.2 LIMITATIONS 37
5.0 REFERENCES 38

LIST OF FIGURES

Page

Figure 1. Ocean current flowchart. 6

Figure 2. This figure represents one image in a sequence of AVHRR composite satellite images. 9

Figure 3. This is the second image in the sequence of images discussed in the text. 10

Figure 4. Northwestern coast of the United States overlaid with MCC velocity vectors. 11

Figure 5. GAC and HRPT images of the Australian Coast. 12

Figure 6. GAC and HRPT images of the Californian Coast. 13

Figure 7. Illustration of the MCC process. Domingues (1999). 14

Figure 8. SST imagery of Tasmania with surface current vectors overlaid. Purple – SST, Black – Chlorophyll 16

Figure 9. Ocean color imagery of Tasmania with surface current vectors overlaid. Purple – SST, Black – Chlorophyll. 17

Figure 10. Location map of MCC current velocity studies. 23

Figure 11. Southeast coast of Australia. Black vectors – MCC currents, White vectors – TOPEX geostrophic currents perpendicular to the ground tracks. 25

Figure 12. Southeastern coast of Australia. Black vectors – TOPEX anomaly velocity, white vectors – geostrophic currents perpendicular to the ground tracks. 26

Figure 13. SST imagery of La Plata River, South America. MCC current velocity vectors overlaid. 27

Figure 14: SST imagery of La Plata River, South America. MCC current velocity vectors overlaid. 27

Figure 15. Ten-day composite of MCC current velocities with inlay of ten-day sea surface height from TOPEX/Poseidon. 21 Sept 96 29

Figure 16. Ten-day composite of MCC current velocities with inlay of ten-day sea surface height from TOPEX/Poseidon. 24 Apr 96 30

Figure 17. Ten-day composite of MCC current velocities with inlay of ten-day sea surface height from TOPEX/Poseidon. 1 Aug 96 31

LIST OF TABLES

Page

Table 1. Small portion of the correlation results from utilizing the MCC method on the imagery in Figures 2 and 3. 15

GLOSSARY OF ACRONYMS

ATBD	Algorithm Theoretical Basis Document
AVHRR	Advanced Very High Resolution Radiometer
BT	Brightness Temperature
CODAR	Coastal Radar
CPU	Central Processing Unit
CTD	Conductivity, Temperature, Depth profiler
EDR	Environmental Data Record
IR	Infrared
MCC	Maximum Cross-Correlation
NPOESS	National Polar-orbiting Operational Environment Satellite System
OI	Optimally Interpolated
OTHR	Over-the-Horizon Radar
SeaWiFS	Sea-viewing, Wide Field-of-View Sensor
SST	Sea Surface Temperature
VIIRS	Visible/Infrared Imager/Radiometer Suite
VIS	Visible
WOCE	World Ocean Circulation Experiment

ABSTRACT

This is the updated version of the Algorithm Theoretical Basis Document (ATBD) for the Ocean Current Environmental Data Record (EDR) derived product of the National Polar-orbiting Operational Environmental Satellite System (NPOESS) Visible/Infrared Imager/Radiometer Suite (VIIRS). The Ocean Current EDR is a derived product because it is determined from input of other VIIRS products such as Sea Surface Temperature (SST) and ocean color. The process addressed in this document has been developed to satisfy the requirements of the VIIRS Sensor Requirements Document (SRD), Version 2 Revision a.

This document describes the theoretical basis and development process of the ocean current algorithm. The algorithm described is the maximum cross-correlation (MCC) method. The MCC method is a semi-automated objective technique used to calculate advective surface velocities from SST imagery. This is a robust, widely used technique that has been used for different applications. It can be applied to any image sequence in time of ocean color, visible, near IR, thermal IR and passive microwave. This procedure calculates the MCC between two successive images by utilizing a small template window within Image One and a larger search window in Image Two (Emery *et al.*, 1986). The location of the MCC coefficient within Image Two defines the end point of a velocity vector that originates at the center of the search window in Image Two. The time interval between the two images and the position of the maximum value is used to calculate a velocity vector field. This technique is repeated for the entire image to determine the overall surface flow. This document presents the algorithm theoretical basis, input data requirements, EDR plan and validation. This document is Version 3 of the Ocean Current ATBD.

1.0 INTRODUCTION

1.1 PURPOSE

This Algorithm Theoretical Basis Document (ATBD) describes the algorithm used to determine ocean surface current velocities from sea surface temperature and ocean color data generated from algorithms processing the Visible/Infrared Imager/Radiometer Suite (VIIRS) infrared and visible wavelength bands. The maximum cross-correlation (MCC) method can be applied to any sequential image set of ocean color, visible, near IR, thermal IR and passive microwave. It has been utilized with passive microwave (all channels) to calculate sea ice motion. A modified version of the MCC method is used for the Sea Ice Age/Edge Motion EDR, see [V-25]. The MCC method is a semi-automated objective technique used to calculate advective surface velocities from sequential sea surface temperature (SST) and ocean color imagery. This procedure utilizes a small template window within Image One and a larger search window in Image Two to calculate the piecewise MCC between two successive images (Emery *et al.*, 1986). The location of the MCC coefficient within Image Two defines the end point of a velocity vector that originates at the center of the search window in Image Two. The time interval between the two images and the position of the maximum value are used to calculate a velocity vector field. This technique is repeated for the entire image to determine the overall surface flow (Tomakian *et al.*, 1990; Kelly and Strub, 1992; Fowler, 1995; Svejkovsky, 1988; Emery *et al.*, 1992; Wu *et al.*, 1992, Garcia and Robinson, 1989).

1.2 SCOPE

This document covers the algorithm theoretical basis for the ocean current Environmental Data Record (EDR). Section 1 describes the purpose and scope of the document. Section 2 provides an overview of the experiment. The processing concept and algorithm descriptions are presented in Section 3. Section 4 summarizes assumptions and limitations. References for publications cited in the text are given in Section 5.

1.3 VIIRS DOCUMENTS

A number in italicized brackets, e.g., *[V-1]* indicates reference to VIIRS documents.

[V-0]	VIIRS Experiment Overview
[V-1]	Imagery
[V-2]	Sea Surface Temperature
[V-3]	Soil Moisture
[V-4,5]	Aerosol Optical Thickness & Particle Size Parameter
[V-6]	Suspended Matter
[V-7]	Cloud Base Height
[V-8]	Cloud Cover/Layers
[V-9]	Cloud Effective Particle Size

[V-10]	Cloud Optical Thickness
[V-11,12,13]	Cloud Top Height, Pressure, And Temperature
[V-14]	Albedo (Surface)
[V-15]	Land Surface Temperature
[V-16]	Normalized Difference Vegetation Index
[V-17]	Snow Cover/Depth
[V-18]	Vegetation Index/Surface Type
[V-19]	Ocean Currents (Near Shore/Surface)
[V-20]	Fresh Water Ice
[V-21]	Ice Surface Temperature
[V-22]	Littoral Sediment Transport
[V-23]	Net Heat Flux
[V-24]	Ocean Color/Chlorophyll
[V-25]	Sea Ice Age And Edge Motion
[V-26]	Mass Loading (IORD Name: Turbidity)
[V-27]	Atmospheric Correction Over Ocean
[V-28]	Atmospheric Correction Over Land
[V-29]	Cloud Mask

1.4 REVISIONS

The original version of this document was dated July 16, 1998. The third revision was dated May 2000. In the third version results were updated and additions were made to the theoretical description, error budget, and validation sections. This is the fourth revision of this document, dated May 2001. No significant changes have been made to this version.

2.0 EXPERIMENT OVERVIEW

2.1 OBJECTIVES OF OCEAN CURRENT RETRIEVALS

Knowledge of the surface currents of the ocean is essential to understanding and working with the ocean environment. A central focus of modern physical oceanography is in defining and refining the general surface circulation of the oceans. Unfortunately, our ability to observe and measure the surface currents of the world's ocean has not progressed very much in the last century. Much of our knowledge of the world's surface currents is based on the "drift" of sailing vessels as part of their daily navigation procedure. German and Norwegian physical geographers and physical oceanographers (Schott, 1942; Sverdrup *et al.*, 1941) summarized these "drift" currents in the 1930s. All of these earlier drift data were developed when navigation was primarily celestial and entailed a fairly large error. These same measurements were used more recently (Wyrtki *et al.*, 1976) to examine the global patterns of mesoscale "eddy energy." Still others, (e.g., Richardson, 1982) have used the individual drift currents to study the past behavior of the Gulf Stream.

Today's ships are much more powerful in their propulsion than their predecessors, however, they are still subject to the forces of these currents. The travel routes of merchant vessels could be made much more efficient if a continuous mapping of surface currents were available. It is surprising that, despite our advanced technology, no system, either satellite or terrestrial, exists to provide us with daily maps of sea surface currents. However, some recent studies have shown that it is possible to map ocean coastal currents by computing the surface current speed and direction from a set of sequential satellite images of sea surface temperature (Emery *et al.*, 1986; Tomakian *et al.*, 1990; Kelly, 1989). Also, satellite altimeter data can be used to map near real-time geostrophic surface currents.

Both local and international marine fisheries could benefit greatly from detailed knowledge of surface currents. Not only do the currents influence travel, but they also affect net setting for fishing and reflect surface features that indicate subsurface fronts known to be associated with increases of fish abundance. Today, both sport and commercial fishermen use daily satellite SST maps to locate fish populations.

The speed and direction of surface currents also affect Naval and Coast Guard operations. Surface currents caused by winds, tides, and sea surface slope can exceed four knots. Four knot currents are unusual, occurring only when the geostrophic, wind-driven, and tidal currents are all in the same direction. These great speeds can affect coastal navigation, explosive ordnance disposal operations, drifting mines, and sonobuoy pattern integrity. Search and rescue operations in particular are dependent upon our knowledge of surface currents, yet our present knowledge of currents derives from wind-driven models that simulate only surface currents due to wind forcing. It would be much better if a daily map of the true surface currents could be provided to agencies in order to predict the movements of subjects they wish to rescue.

2.2 INSTRUMENT CHARACTERISTICS

The VIIRS sensor is being designed based on the VIIRS Sensor Requirements Document (SRD) of the National Polar-orbiting Operational Environment Satellite System (NPOESS), and on EDR thresholds and objectives.

Other instrument data (SST, ocean color) are used to compute the ocean current EDR. The SST and ocean color are not operated simply to compute currents, but have other purposes as well. Please refer to *[V-2]* and *[V-24]*.

2.3 RETRIEVAL STRATEGY

This sensor is not designed to measure currents. Instead, a method to use available sensor data (SST and ocean color) to infer the surface currents is invoked. Please refer to [*V-2*] and [*V-24*].

3.0 ALGORITHM DESCRIPTION

In the MCC method, the basic assumption is made that all changes in SST patterns are due to horizontal advection by the surface currents. This same assumption can be invoked when looking at visible images of cloud cover, passive microwave images of sea ice, infrared (IR) images of sea surface temperature, or visible images of ocean color. The simple, robust technique used to determine sea surface currents from satellite imagery data is called the maximum cross-correlation method (Ninnis *et al.*, 1986; Emery *et al.*, 1986; Tomakian *et al.*, 1990; Emery *et al.*, 1992; Kelly and Strub, 1992; Kamachi, 1989). The assumption of linear advections requires that advective changes take place more rapidly than those due to heating/cooling or upwelling/downwelling (the competing mechanisms changing SST). There are many locations where this clearly will not be valid. Applications of MCC to areas of strong upwelling, such as the near-shore West Coast of the United States, will not work in summer when upwelling is strong. Regions of vigorous heat flux also will be a problem. In addition, the method requires an observable ocean surface gradient. Therefore, isothermal regions, as found in the cores of strong western boundary currents, will not work with the MCC method.

To minimize these problems one has to use images close together in time so that heating and cooling (or upwelling/downwelling) do not have a long time to occur. Time intervals between images must range from 4 to 24 hours. After 24 hours, the numerical noise builds up in the calculation causing the MCC currents to deviate from the truth currents in numerical simulations (Emery et al., 1992). Also, to account for the linear requirements, small template and large search windows that will resolve most of the curvature as small linear segments must be used. At the same time it is important to have template windows large enough for each correlation coefficient to be statistically significant based on the number of points in each template window. For 1 km resolution images separated by less than 24 hours, a practical template window size was found to be 40 x 40 km. Biological production and chemical dissolution lead to ocean color image changes that contradict the assumption of linear advection for ocean color images. These effects also have somewhat longer time scales and are small when image intervals are between 4 and 24 hours. A problem with testing the MCC on present ocean color imagery is the fact that the present SeaWiFS imager only repeats coverage every 24 hours. Perhaps the combination of MODIS and SeaWiFS will make it possible to evaluate better the MCC method for ocean color applications.

The SST and ocean color data are used in the MCC method to determine the speed and direction of the ocean surface current. The calculated SST is defined as the representative temperature value for the first 1 mm of the water column. The visible part of the spectrum (ocean color) could be used to obtain data to approximately a few cms deep. In this case, one must assume that the currents in the ocean skin and at 1 mm are similar which is likely to be an excellent assumption. Recent studies (Emery *et al.,* 1998) have shown that the main reason to use both SST and ocean color is to increase the sample size in order to reduce the effects of clouds. Obviously, this assumes that the ocean color data comes from a different satellite crossing at a slightly different time. This is not the case for NPOESS VIIRS, which will obtain data for ocean color and SST retrievals at the same time. It is very important to recognize that the noise factors in the ocean color imagery are completely different from those for the SST imagery. The reason to blend thermal MCC velocity vectors with color MCC currents is to improve the sampling. This will be true of VIIRS since the channels will be sensing two completely different surface patterns which should be altered by the currents in the same way. Thus, both methods should

give the same currents. The only thing that would benefit from them being on different satellites is that the clouds would move between them. This will not be the case with different VIIRS channels.

3.1 PROCESSING OUTLINE

The MCC currents depend on data from other VIIRS sensor components. Thus, their processing is tightly coupled to the computation of the target parameters (i.e., SST and ocean color). See Figure 1 for a flowchart of the MCC process.

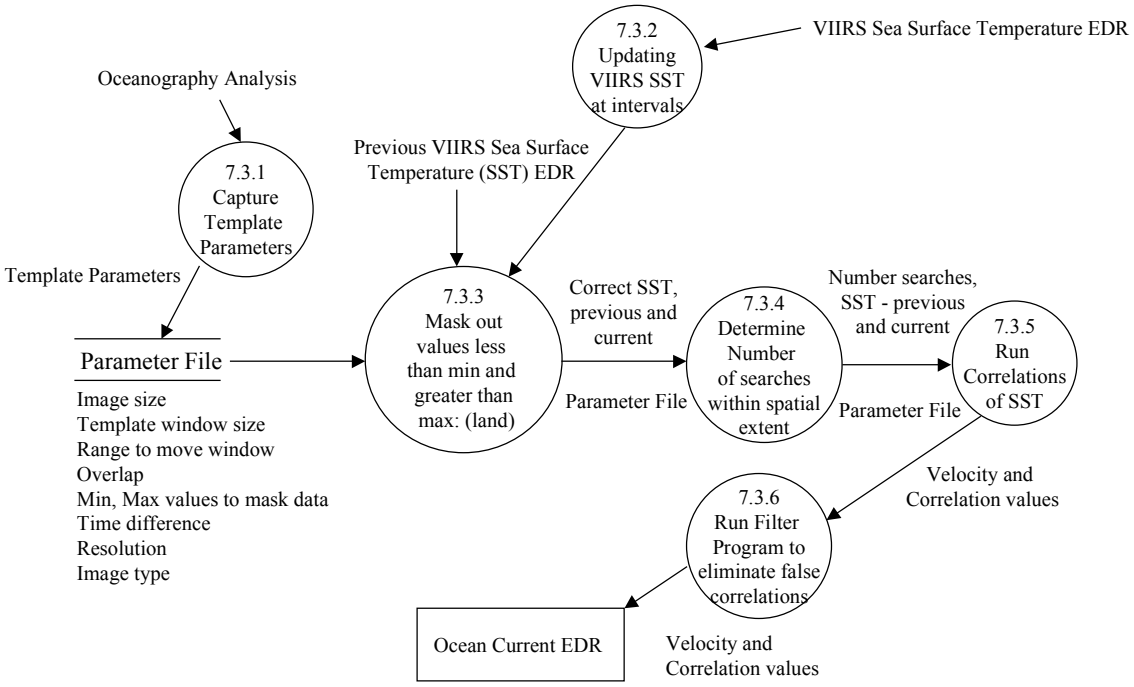

VIIRS Ocean Current EDR Level 2 Data Flow Diagram

Figure 1. Ocean current flowchart.

3.2 ALGORITHM INPUT

3.2.1 VIIRS Data

The targets are SST from the IR channels and ocean color from the VIS channels. As accurate image navigation is essential, cloud removal, which can change the pattern, is important. In cloudy conditions, one can find coincident clear spots, compute the vectors, and then composite the vectors over time. One should not composite the SST or ocean color images and then compute MCC currents. The accuracy of the cloud removal is important only for absolute identification. The absolute magnitude of the radiance is not of great importance, the main interest is in its distribution in space (i.e., its pattern).

An alternative approach to obtaining the MCC surface currents is to use the calibrated brightness temperatures. The same requirements on the SST and ocean color input are also placed on the BT data set, i.e., cloud removal and navigation.

3.2.2 Non-VIIRS Data

Only VIIRS SST and ocean color data, and possibly brightness temperature, will be utilized in generating output for the ocean current EDR.

3.3 THEORETICAL DESCRIPTION OF OCEAN CURRENT RETRIEVALS

3.3.1 Physics of the Problem

The algorithm is based on the maximum of the cross-correlation. Competing algorithms have minimized the differences between Image One and Image Two, but the results are no better than with the cross-correlation technique, and the differences take longer to compute at the same rate. Thus, these competing algorithms offer no advantages. As shown in Table 1, some cross-correlation fields are not markedly single valued in terms of the maximum correlation. This is the reason that methods such as relaxation have been developed. However, it is difficult to show a dramatic improvement when compared to the simple MCC method.

The MCC method is a semi-automated objective technique used to calculate advective surface velocities from SST imagery. This method is semi-automated because the retrieval of an optimal current field requires subjective decisions in terms of selecting the template window size, the search window size, the amount of filtering (cut-off value, next-neighbor limits) and smoothing. Thus, the method is not totally objective. The computation does not require operator intervention for each vector, but there are some very important subjective aspects to the calculation. The selection of the template and search window requires a prior general knowledge of the current field being mapped. This procedure calculates the MCC between two successive images by utilizing a small template window within Image One and a larger search window in Image Two (Emery *et al.*, 1986). The location of the MCC coefficient within Image Two defines the end point of a velocity vector that originates at the center of the search window in Image Two. The time interval between the two images and the position of the maximum value are used to calculate a velocity vector field. This technique is repeated for the entire image to determine the overall surface flow. Emery et al. (1986, 1992) and Garcia and Robinson (1989) give additional details about the MCC method.

Emery *et al.* (1986) determined that applying the MCC method to the satellite infrared temperature imagery yielded small MCC values and incoherent flow patterns. Therefore, the technique was applied to the SST gradients that resulted in a more coherent velocity field. However, recent studies by Emery *et al.* (1992), Kelly and Strub (1992), Wu *et al.* (1992), Fowler (1995), and Garcia and Robinson (1989) have disproved the findings of Emery *et al.* (1986). Studies have shown that the gradient images are very noisy and do not produce a more coherent surface velocity field, as previously thought. Thus, for the ocean current EDR, the SST imagery will be utilized.

In its most basic formulation, the MCC method does not do an adequate job in determining rotational and deformational motion. Emery *et al.* (1986) used a time period between successive images of 4 to 5 hours because the rotational motion can be approximated as translational. If a

longer time period is employed as Emery *et al.* (1986) suggested, the velocity vector field would not reliably represent the rotational movement. Kamachi (1989) formulated the MCC problem in such a way that it explicitly accounted for rotational motion. Other solutions for rotational motion require detailed knowledge of the location of the circulation features which does not allow for an automated process to compute surface currents.

Spatial resolution has proven to be a problem when using the MCC method. For the maximum cross-correlation method to work, we have to have 1 km or smaller resolution at nadir. To clarify, the method will "work" with any spatial resolution, since the MCC method merely needs two arrays of data to perform the calculation. However, the problems with spatial resolution do not have anything to do with the MCC method, but rather with the geophysical process that is being estimated. In other words, the method is limited when the results do not really correspond to anything that is considered realistic. Past studies by Emery *et al*. (1986), Emery *et al*. (1992), and Fowler (1995) have shown that coarser image resolution produces greater errors in the MCC velocity vectors produced. Studies by the VIIRS ocean group have verified these findings, by utilizing the MCC method on 1 km and 4 km resolution imagery. See Figures 2, 3, and 4, and Table 1.

The images in Figures 2 and 3 are 4 km 5 day composite images of the East Coast of the United States from March 1985. No MCC vectors are overlaid because the correlation values are essentially the same value: 0.999999. These images are displayed to illustrate that the MCC method does not work for imagery that has been composited, as well as for 4 km resolution and large time scales.

Figure 4 displays the ocean current vectors generated from the MCC method. The vectors are overlaid on the second image of a sequence of images depicting the northwestern coast of the United States. The images are from AVHRR data taken in September 1995. These images utilized in the MCC algorithm are separated by 5.5 hours and have a resolution of 1 km. The smaller temporal and spatial scales are necessary for the MCC method to be utilized. The right hand side of the image is black representing the land cover mask for the northwestern United States coast. Directly adjacent to the coast, an upwelling event is evident. The lower left hand corner of the image is covered by clouds.

Table 1 displays a small portion of the correlation results from utilizing the MCC method on the imagery in Figures 2 and 3, specifically the South Atlantic Bight region. The high correlation values obtained illustrate the fact that the large spatial and temporal scales greatly affect the utilization of the MCC method. The entire data set for the region also consisted of MCC values as large as those recorded here.

Images in Figures 5 and 6 also display the spatial resolution problem in determining the MCC velocity vectors. These figures depict HRPT and GAC images for two oceanographic coastal regions: eastern Australia and California. The difference between the GAC and HRPT velocities is consistent with the loss of resolution of the GAC data. The maximum velocity for the Australian waters is 35 cm/s (Figure 5). These images are eight hours apart on 29 September 1998. The maximum velocity for the Californian waters is 15 cm/s with a time interval between the images of 13 hours on day 326, 1999 (Figure 6).

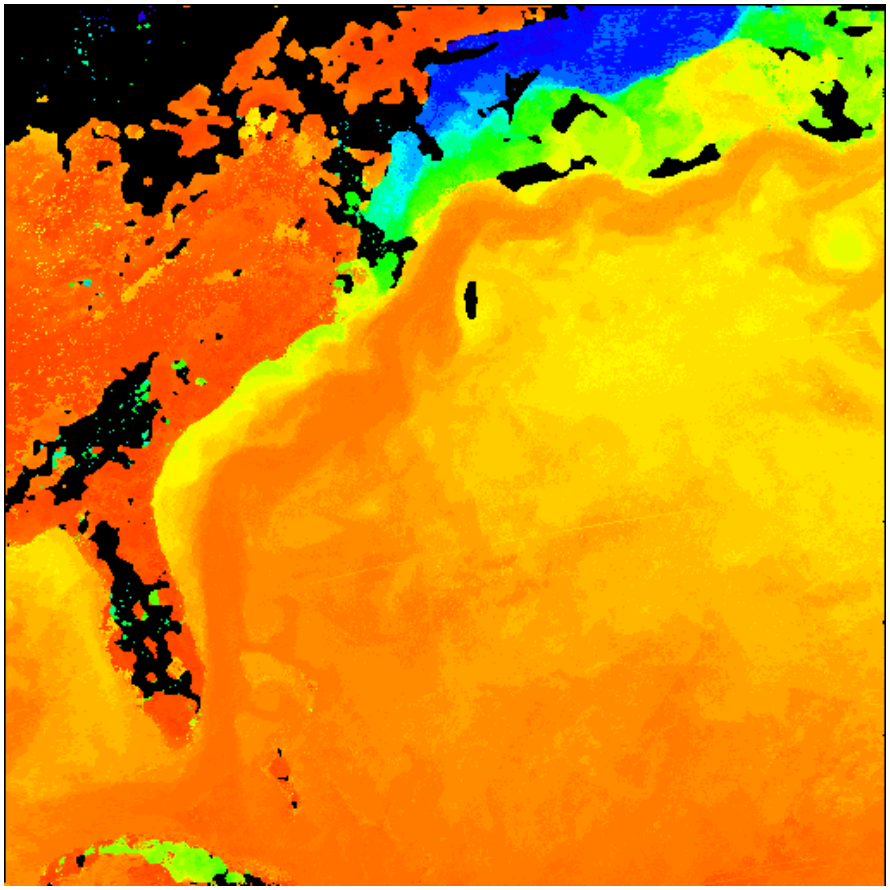

Figure 2. This figure represents one image in a sequence of AVHRR composite satellite images.

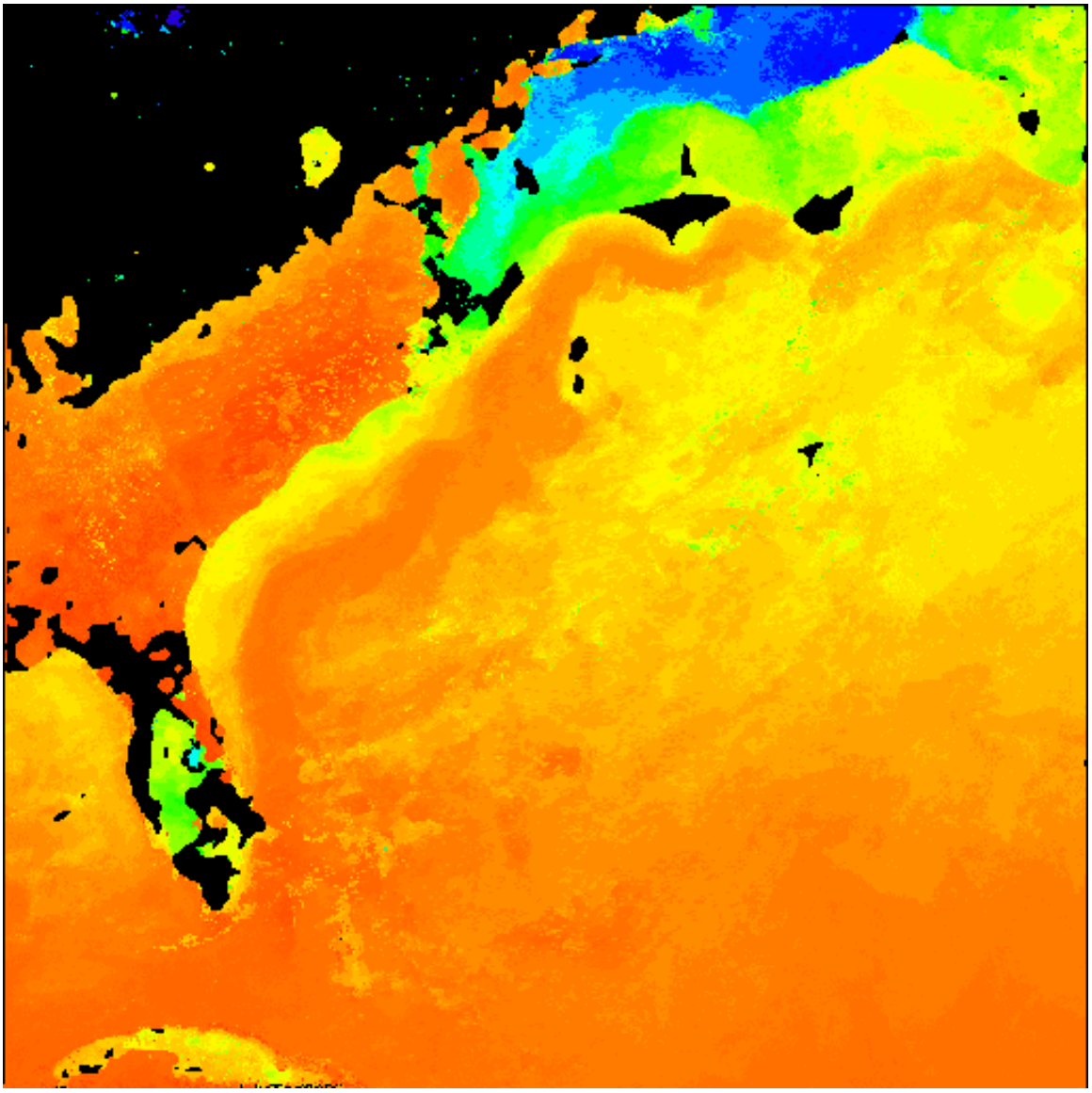

Figure 3. This is the second image in the sequence of images discussed in the text.

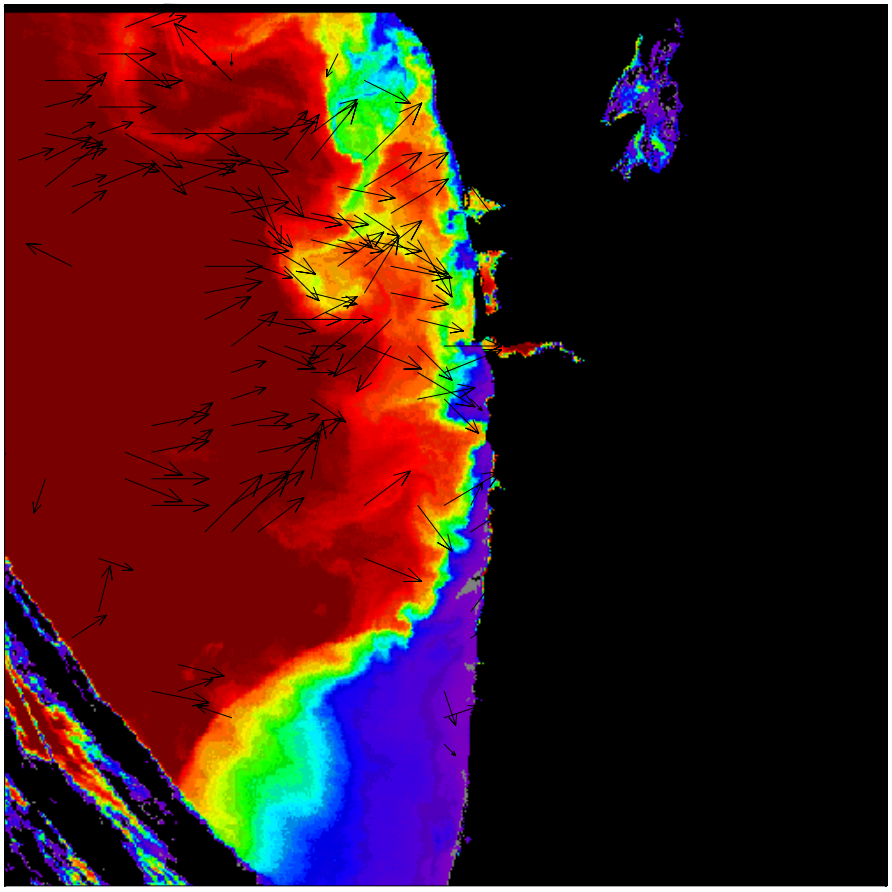

Figure 4. Northwestern coast of the United States overlaid with MCC velocity vectors.

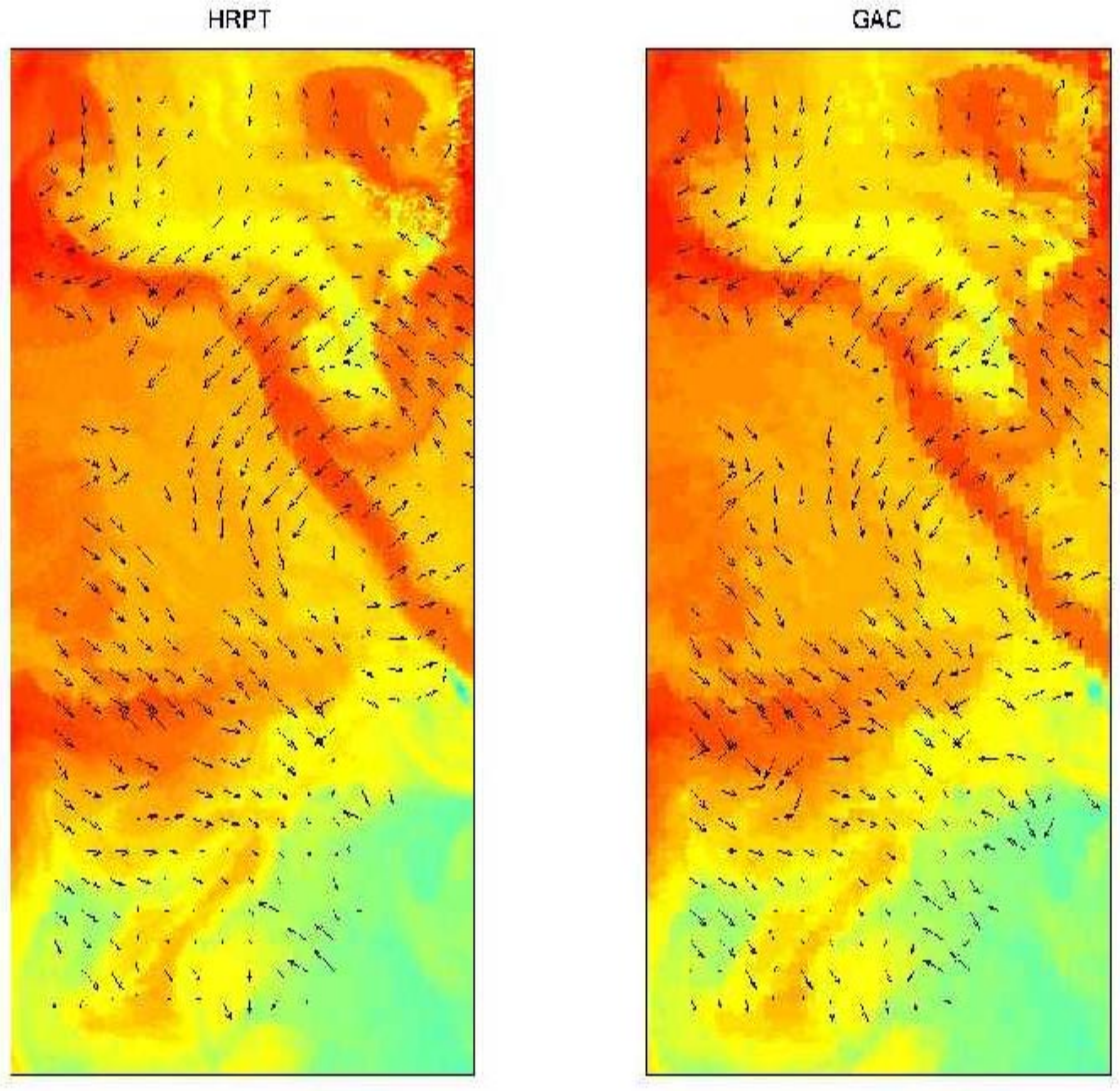

Figure 5. GAC and HRPT images of the Australian Coast.

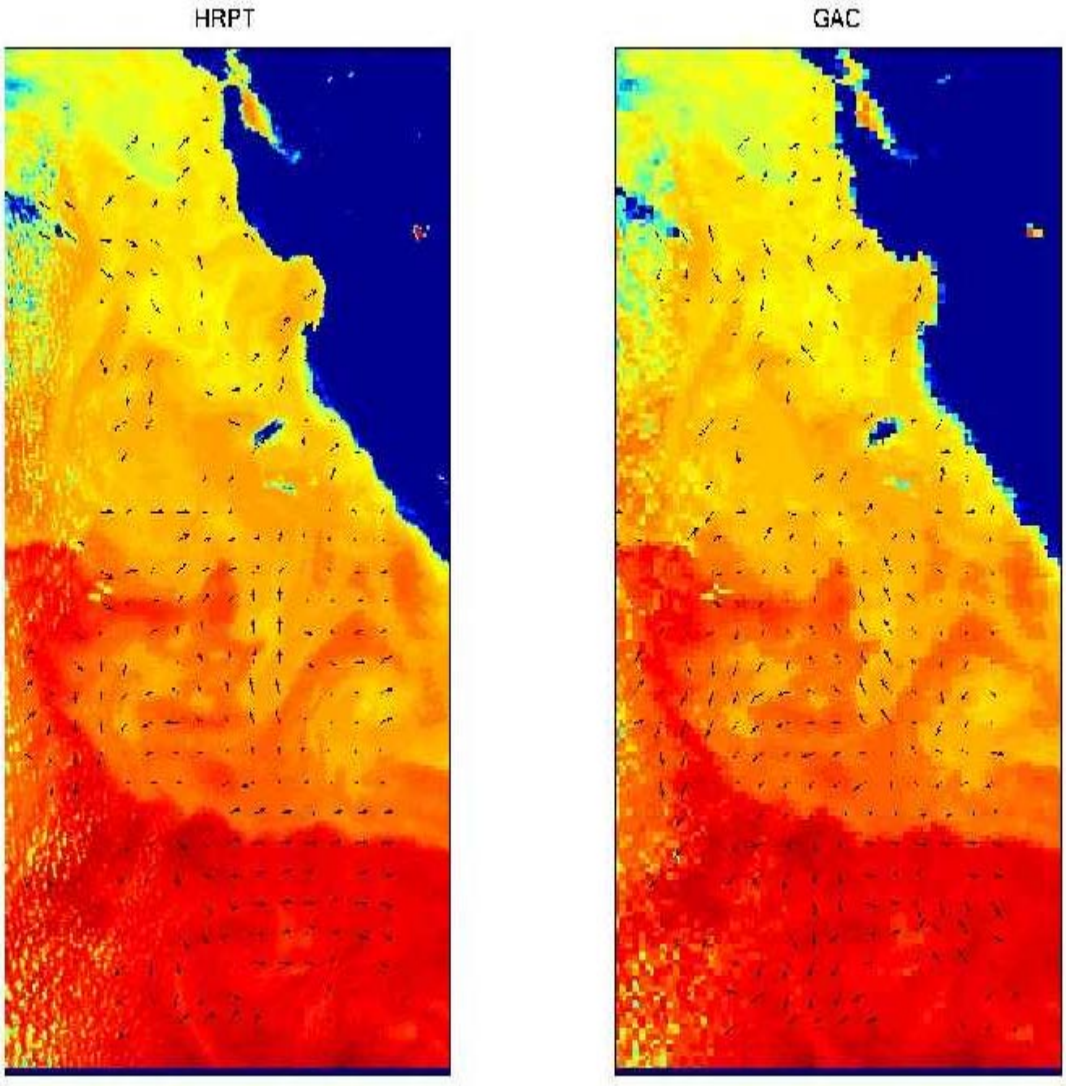

Figure 6. GAC and HRPT images of the Californian Coast.

The size of the search window in Image Two is determined to be the resultant maximum displacement from Image One to Image Two and the expected surface velocities that produced the displacement (Kelly and Strub, 1992). If the size of the subregion used to conduct pattern matching is too large, the detailed flow structure can be lost and the resulting velocity field may be incorrect. However, if the window size is too small, the confidence level in the velocity results will be very small. A large search area can be used to resolve the rotational motion sufficiently. Kelly and Strub (1992) determined that within areas of very intense flow, the MCC method largely underestimates the velocity field. Prior knowledge of the basic current field is needed to choose the right processing parameter (windows, filters, etc.). The isothermal regions of the strongest currents easily explain the estimates in the western boundary current region. The MCC method would not work at all in this region, thus biasing the method toward an underestimate of the currents. The most important thing to do is to accommodate the maximum velocity for a region. Hence, the software really needs to be adaptive using larger search windows for larger velocities. This also depends on the interval between the images, with shorter intervals being matched with smaller search windows. Figure 7 shows the process of the MCC method (Domingues, 1999). The center point of the subimage, (X_{mcc}, Y_{mcc}), that produces the maximum correlation coefficient is the endpoint of a motion vector with its origin at the center of the search window (X_c,Y_c).

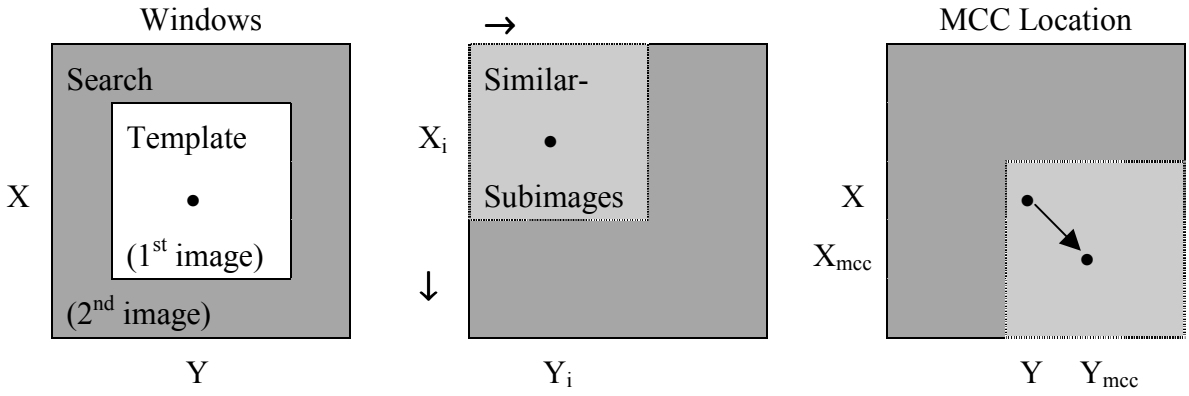

Figure 7. Illustration of the MCC process. Domingues (1999).

Table 1. Small portion of the correlation results from utilizing the MCC method on the imagery in Figures 2 and 3.

MCC Value	Pixel Location
0.9999990	(143,196)
0.9999990	(142,207)
0.9999989	(136,211)
0.9999989	(137,213)
0.9999987	(144,196)
0.9999987	(154,203)
0.9999987	(151,204)
0.9999987	(144,136)
0.9999987	(136,213)
0.9999987	(135,214)

Figures 8 and 9 illustrate the importance of utilizing the ocean color and SST measurements to infer the MCC surface current velocity. There should be much stronger current velocities in this area. However, they cannot be resolved over 24 hours. Detailed information about the SST and ocean color measurements was addressed in the algorithm description section, Section 3.0. The imagery clearly demonstrates the ability of the ocean color MCC current vectors to complement the SST MCC current velocity vectors (Emery, 1998).

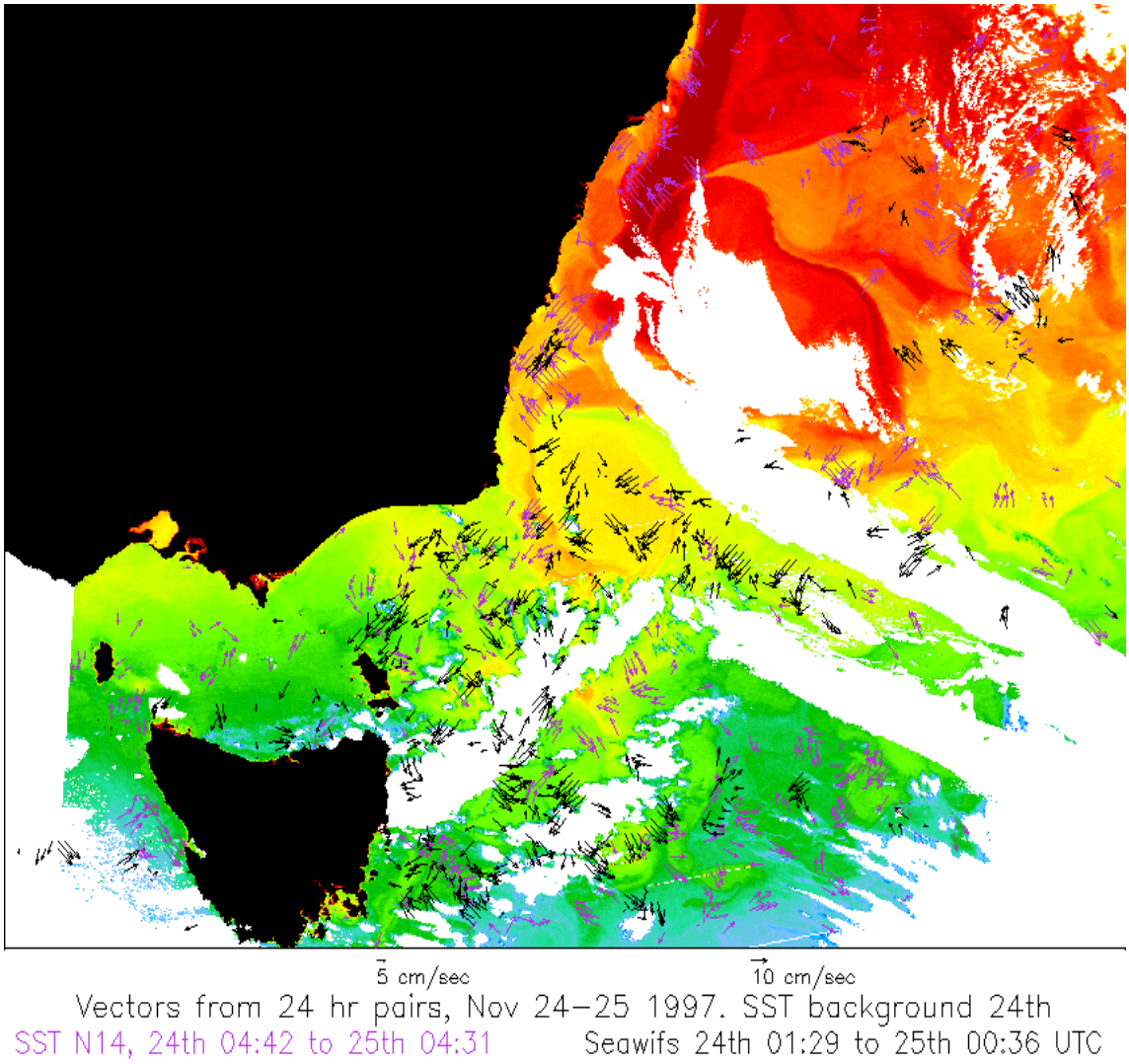

Figure 8. SST imagery of Tasmania with surface current vectors overlaid. Purple – SST, Black – Chlorophyll

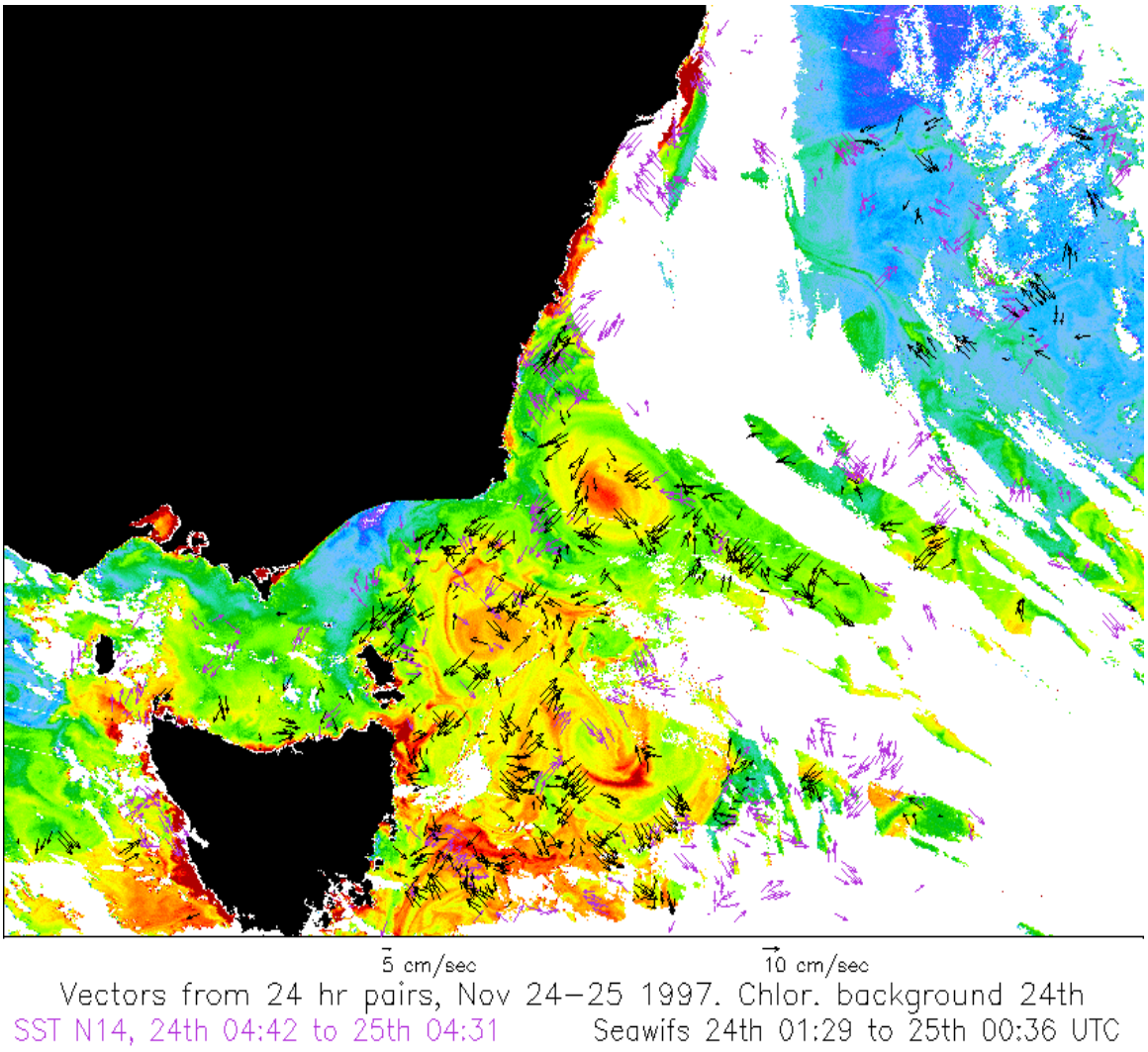

Figure 9. Ocean color imagery of Tasmania with surface current vectors overlaid. Purple – SST, Black – Chlorophyll.

Currently, the baseline approach to inferring the MCC surface currents is the utilization of SST. As long as the quality of the SST data is very good, this will remain as the main approach. At the present, VIIRS SST studies show that with the use of different algorithms the calculation of SST has improved greatly compared to the AVHRR SST measurements. The accuracy in temperature is much greater and the overall error has decreased. (Please refer to the VIIRS SST document [V-2] for further information.) It is justified from these analyses that the VIIRS SST approach should be the baseline for inferring the MCC surface current

An alternative approach to determining the MCC ocean currents, rather than utilizing SST and ocean color, is to use the calibrated brightness temperatures (BT). To use the brightness temperature approach, the 11-micron channel should be used because it is the most responsive and has the best atmospheric window. For the ocean color channel, 412 would be the best. The BT image would give the appropriate pattern and must be calibrated and navigated accurately. Here, the interest lies in only the BT temperature pattern and not the absolute temperature.

Past work has been done on BT and AVHRR SST imagery. It has been shown that it is better to use BT rather than SST when utilizing the present day SST algorithms. Currently, the differencing of the two similar values generated by the SST algorithm accentuates the noise in each of the individual channels. It is this noise that results in poorer cross correlation values using the SST fields.

Dr. Barton did a study near Tasmania in which the data showed that there were more than twice as many high correlations with SST than BT (Emery, 1999) This leads to the conclusion that the errors in SST are going to be much greater than those with the BT. However, these analyses were performed on AVHRR SST imagery and not the new corrected VIIRS SST data set. The VIIRS SST data greatly decreases the errors affecting the MCC current vector velocities. With the proposed VIIRS dual split window approach in determining SST, the noise is greatly reduced and the cross correlation values generated are reasonable.

3.3.2 Mathematical Description of the Algorithm

As stated earlier, the MCC method is a semi-automated, objective technique applied to sequential SST and ocean color imagery in order to determine surface current velocities. It is a well-established technique used to derived the displacement of features in a series of sequential images. Ninnis *et al.* (1986) has described the MCC method in great detail. The following description of the mathematics behind the MCC method comes from Ninnis *et al.* (1986).

The MCC method for determining velocities is best explained by determining the relative spatial lag between a pair of two-dimensional functions. Consider two signals f(x, y) and g(x, y) defined over the region |x| < L, |y| < L and related by a vector lag (x_0, y_0):

$$f(x,y) = g(x+x_0, y+y_0) \tag{1}$$

The auto and cross-covariance functions are:

$$r_{ff}(x',y') = E[(f(x,y)-m_f)(f(x+x',y+y')-m_f)]$$

$$r_{fg}(x',y') = E[(f(x,y)-m_f)(g(x+x',y+y')-m_g)]$$

where E[ ] is the expected value and m_f, m_g are the signal means:

$$m_f = E[f(x,y)]$$

$$m_g = E[g(x,y)]$$

The normalized cross-covariance is given by:

$$\rho(x',y') = \frac{r_{fg}(x',y')}{\sqrt{\sigma_f^2 \sigma_g^2}}$$

where the variances of *f* and *g* are:

$$\sigma_f^2 = r_{ff}(0,0)$$

$$\sigma_g^2 = r_{gg}(0,0)$$

At (x_0, y_0) the value of the covariance r_{fg} is:

$$r_{fg}(x_0, y_0) = E[(f(x,y) - m_f)(g(x + x_0, y + y_0) - m_f)] \quad (2)$$

Substituting Equation 1 into Equation 2, we get:

$$r_{fg}(x_0, y_0) = E[(f(x,y) - m_f)^2] = r_{ff}(0,0)$$

Also from Equation 1 the value of *g* at lag (x_0, y_0) is σ_f^2. Hence, the cross-correlation is given by:

$$\rho(x_0, y_0) = \frac{r_{fg}(x_0, y_0)}{\sqrt{\sigma_f^2 \quad \sigma_g^2}} \sqrt{g^2} = 1$$

Once the cross-correlation values have been obtained, the data must be filtered. Emery *et al.* (1991) showed that two filtering methods are needed in order to eliminate the "bad" MCC velocity vectors. One method incorporates a cutoff value for the MCC correlation coefficients. Any MCC velocity vector with an MCC correlation below this cut-off value is ignored (Emery *et al*., 1992). For this study, the cut-off value is 0.6, because it produced better results than other cut-off numbers.

Next-neighbor filtering is the second method used in processing the MCC velocity vectors. This method compares neighboring vector directions in order to determine which are "good" or "bad" vectors (Emery *et al.*, 1992). Emery *et al.* (1992) defined a vector to be "good" only if a portion of its neighboring vectors' differences in their x and y direction is less than a chosen displacement value. This filtering method follows the premise that the displacement of the features contains some spatial auto-correlation. So, if a vector is determined to be "good" for a certain pixel, then its neighbors also will have similar displacement vectors. Increasing the minimum correlation value usually can eliminate the "bad" vectors. Often, when this is done, the "good" vectors are also deleted. In order to keep the "good" vectors with lower correlation values this filtering method must be applied.

The MCC method utilizes a filter file that contains three values. The first value is the minimum required correlation value. The second value represents the minimum number of neighboring pixels with "good" vectors. The last number represents the maximum displacement of x and y for the neighboring vectors in relation to the pixel vector.

3.3.3 Archived Algorithm Output

Many basics must be considered in order to use the MCC method, and, when the method is applied to a longtime series of images, some important additional factors must be considered. Nevertheless, nothing has been found that is clearly "better." The MCC method appears to be the easiest and least expensive option.

Modifications made to the MCC method over time include—

1. *Kamachi's rotation method*: The user must visually identify any eddies and then rotate the template/search axis at those locations. In theory, this should improve the computation more than it actually does. It is a subjective method in that eddies must be visually identified. The MCC obtains most of the rotational current if the template is kept small and the search window large (Kamachi, 1989). Because this method is very subjective, it is recommended that this method not be used. Results show that this rotation method is not better than the MCC method when using large template windows.

2. *The relaxation method*: Cross-correlation fields have multiple maxima. To ensure the selection of the correct maximum, the relaxation method is used. This appears to yield a small but measurable improvement. It has been shown that this method is computationally quite extensive and does not offer a big enough improvement for the effort. Again, the use of this method is not recommended.

3. *Joint-patch least squares matching*: This method is a complete deviation from MCC and uses an error or residual minimization technique. It is slower than the MCC method and appears to give almost identical vectors.

4. *Kelly and Strub*: Kelly and Strub demonstrated that the SST gradient method gives the same results as the MCC method. However, MCC is easier to use.

5. *Tony Liu of GSFC uses "wavelet" to compute ice motion in a method similar to the MCC*. This method is much more involved computationally and requires a subjective selection of the wavelets.

3.3.4 Variance and Uncertainty Estimates

The only way to determine the accuracy of the MCC method is to perform a field program sampling at the same time that the remotely sensed data is being retrieved. This is not a direct method, but rather it uses the assumption that advection takes place between the satellite images. Thus, when uncertainty is applied to the computational method, the accuracy of the cross correlations can be judged and not the inferred ocean surface currents. The MCC velocities have been compared with numerical simulations, shallow conductivity, temperature, depth profiler (CTD) surveys, and drogued drifting buoy tracks (Emery *et al.*, 1986; Emery *et al.*, 1992; Garcia and Robinson, 1989). However, despite these comparisons, it has not been possible to assess the accuracy of the process because conditions change over time and by geographic location. Although all of these comparisons have demonstrated clearly the accuracy of the MCC velocity directions, not enough statistical data have been compiled in order to give a single numerical value to the accuracy of the MCC method. It is important to note that the numerical models were used to test the method and not to evaluate the application of MCC to satellite data.

CTD surveys, satellite altimetry, and XBT data, only can provide estimates of the geostrophic currents which must be part of the MCC currents, but certainly not all of them. The MCC current is some sort of combination or superposition of the geostrophic currents with the wind driven currents, and tidal currents. As a result, it is simply not possible to make precise independent measurements of the currents computed with the MCC method. Drifters also have responses based on where they are drogued and the relationship between the drogue and float.

3.3.4.1 Error Budget

The error budget depends on the "ground truth" measurements. An error budget based on the image location accuracy must be developed, then propagated through the equations. It would be much better if there were some validation data/method to use. The ideal scenario would be to deploy many buoys drogued at different depths ranging from 1 – 50 m. In addition, shallow CTD surveys should be conducted. This would constitute a systematic comparison between the *in situ* data and satellite imagery. Through this we would obtain a better understanding of what velocity the MCC vectors represent, as well as of the accuracy of the MCC method.

Errors in temperature and/or brightness temperature, as well as ocean color, only affect the correlation values obtained but not the MCC surface velocity that is inferred. The error from the SST/BT/ocean color cannot be propagated through to an MCC velocity error. Geolocation is the only main source of error that can be propagated to the MCC surface currents. All that really matters is the temperature/color pattern, not the magnitude of the values. Currently, it is not understood what is happening with the currents and the use of the MCC method. This is the only method to obtain currents from imagery.

The MCC method works when a surface temperature or ocean gradient is present. Areas that undergo strong upwelling/downwelling conditions will not work for the MCC method. Also, heating/cooling regions within the oceans cause problems. However, these events occur over longer time periods so a shorter interval can combat the problem. The MCC method must be used in regions where there are relatively strong surface currents.

Currently, a lot of information and experience has been obtained that demonstrates that it is possible to retrieve some really useful current information under conditions where nothing else can give us the space/time resolution.

It is not reasonable to have an error budget for the ocean currents EDR because this is a derived product. However, there are three error sources that effect the ocean currents EDR. These include SST, clouds and geolocation. The geolocation is an important factor to consider because a sequence of satellite imagery must be used to determine the ocean currents. Thus, it is imperative that the exact location of the imagery is known in order to perform the MCC method.

Because SST is used to determine the ocean current velocity, one would think that an error in the SST would effect the MCC currents. However, this is not the case. The MCC method uses the SST pattern to determine the surface current velocities not the temperatures. If noise is added to the SST from one image to the next, then it is possible to produce a change in the surface pattern making it fuzzier. This would give an error in the matching. So, if you have image one with no noise, then image two with small noise added, then the results would show a velocity with that noise effect added. The SST error cannot be used to find the MCC error.

The third error source is clouds. A cloud mask will be used on the SST data producing an image with clouds masked out. The MCC method does not process areas that are masked. If there is no data, the method goes to the next pixel and performs the correlation again. The clouds in the imagery leave gaps in the data set, producing an error term.

One method to overcome the clouds is to composite the imagery. It has been shown that this method aids in determining/depicting the surface current velocities for an entire region instead of just portions of it. First, find a series of images with small patches without clouds. Then, perform the MCC method on those images. Eventually, an image can be generated by compositing a sequence of these patches over a few days. Compositing is carried out by obtaining the maximum velocity for a specific location.

3.4 ALGORITHM EVALUATION AND SENSITIVITY STUDIES

The algorithm does not lend itself to sensitivity studies because this passive technique can be influenced by non-advective sources of surface property changes. We have to develop a sensitivity testing procedure that takes advantage of the MCC method.

The following important considerations must be taken into account.

1. Utilize vectors with cross-correlations that exceed the 95 percent confidence limit.

2. Design search and template windows to resolve the maximum current and optimize the ratio between search and template (to increase the degrees of freedom).

3. Overlap search windows to give a smooth spatial coverage.

4. Filter next-neighbor errors in space

5. Use multi-pair technique.

6. Use next-neighbor filtering in time as well as space

The first four items apply to any and all images to be analyzed. However, the last two items pertain only to a time series of images.

Below are several examples showing the use of the MCC method to infer ocean surface currents. These examples utilize sequential SST and ocean color imagery to determine the MCC currents.

Figure 10 depicts the regional locations where the MCC method has been applied. It is important to note that the study regions are limited. The reason is that most research has been focused on proving or improving the MCC technique by analyzing the same area again and again, instead of moving to different regions. However, the analyses, so far, have shown the MCC method does a good job at presenting the ocean current, as shown by the agreement with altimeter data and ocean models.

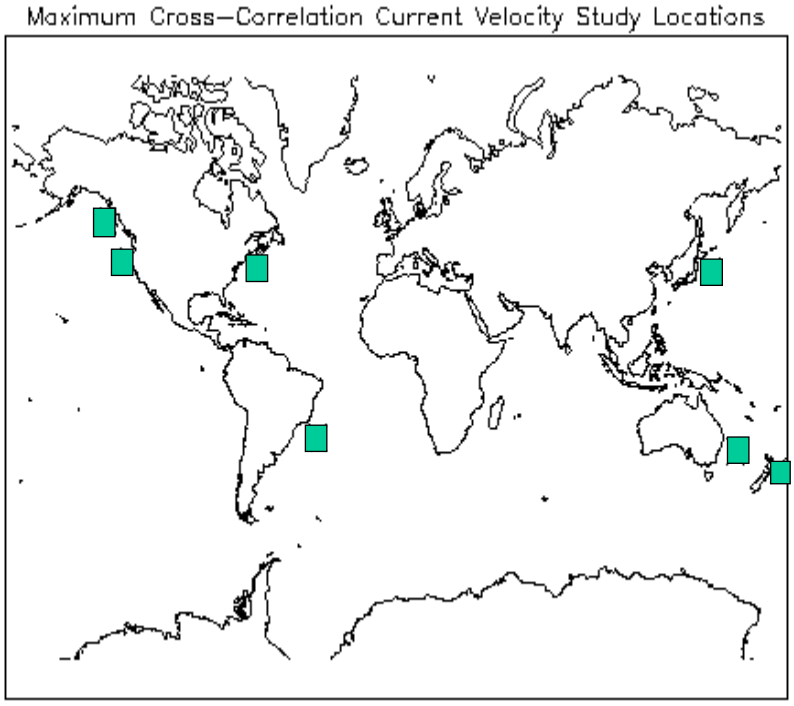

Figure 10. Location map of MCC current velocity studies.

The following images display a good comparison of the MCC surface velocities with altimeter geostrophic currents. The MCC velocities that were inferred from SST imagery off the Southeast Australian coast have been optimally interpolated (OI) to a point stream function (Figure 11). It is this last restriction that makes the field smooth with no singularities. Figure 12 shows the TOPEX anomaly velocity. This is the deviation of a specific ground track from a mean surface. It can be seen in these two figures that there is great agreement between the two surface current measurement methods.

Figure 12 illustrates the very close agreement between the TOPEX data and the MCC surface currents. This is especially represented near the northern tip of Tasmania.

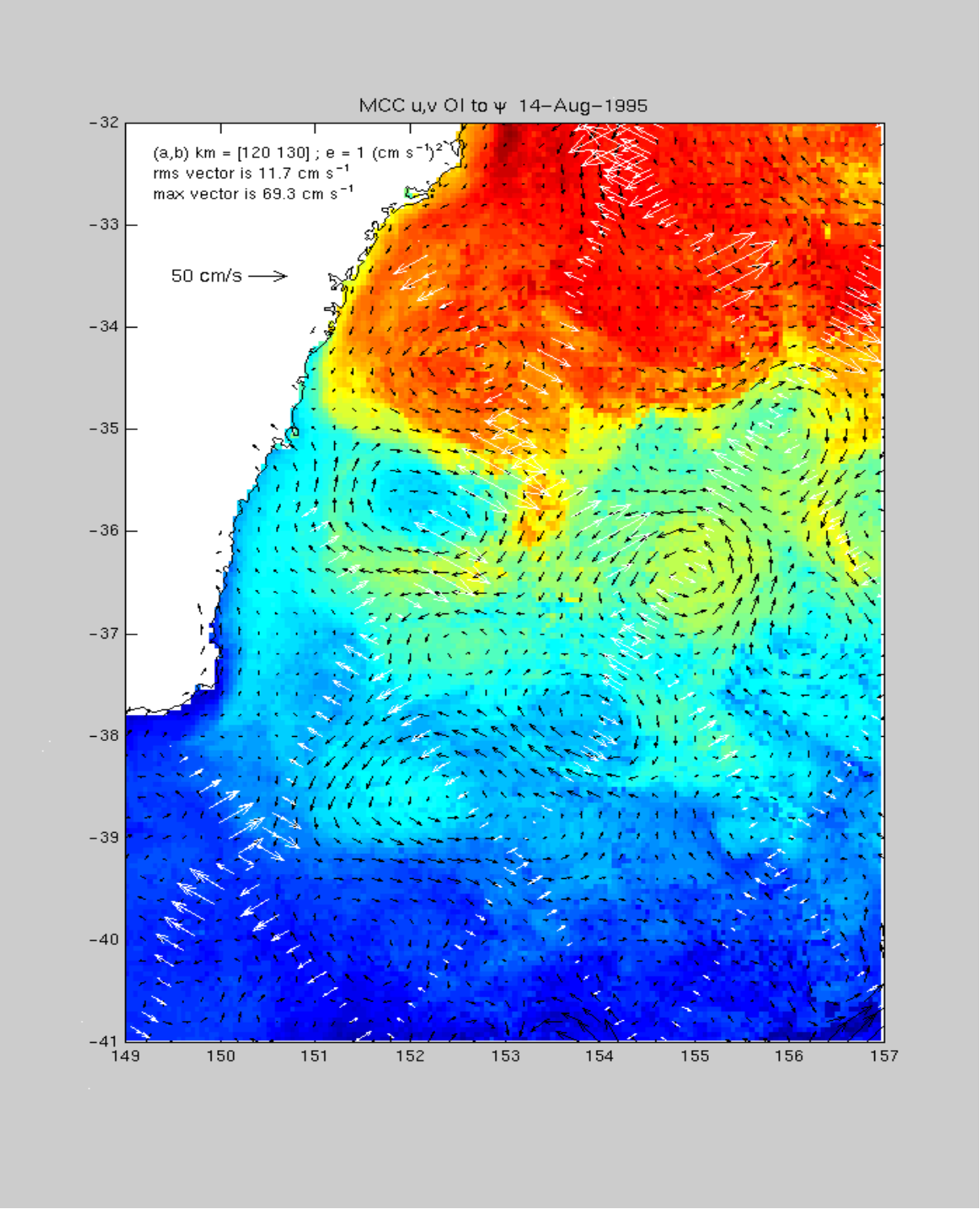

Figure 11. Southeast coast of Australia. Black vectors – MCC currents, White vectors – TOPEX geostrophic currents perpendicular to the ground tracks.

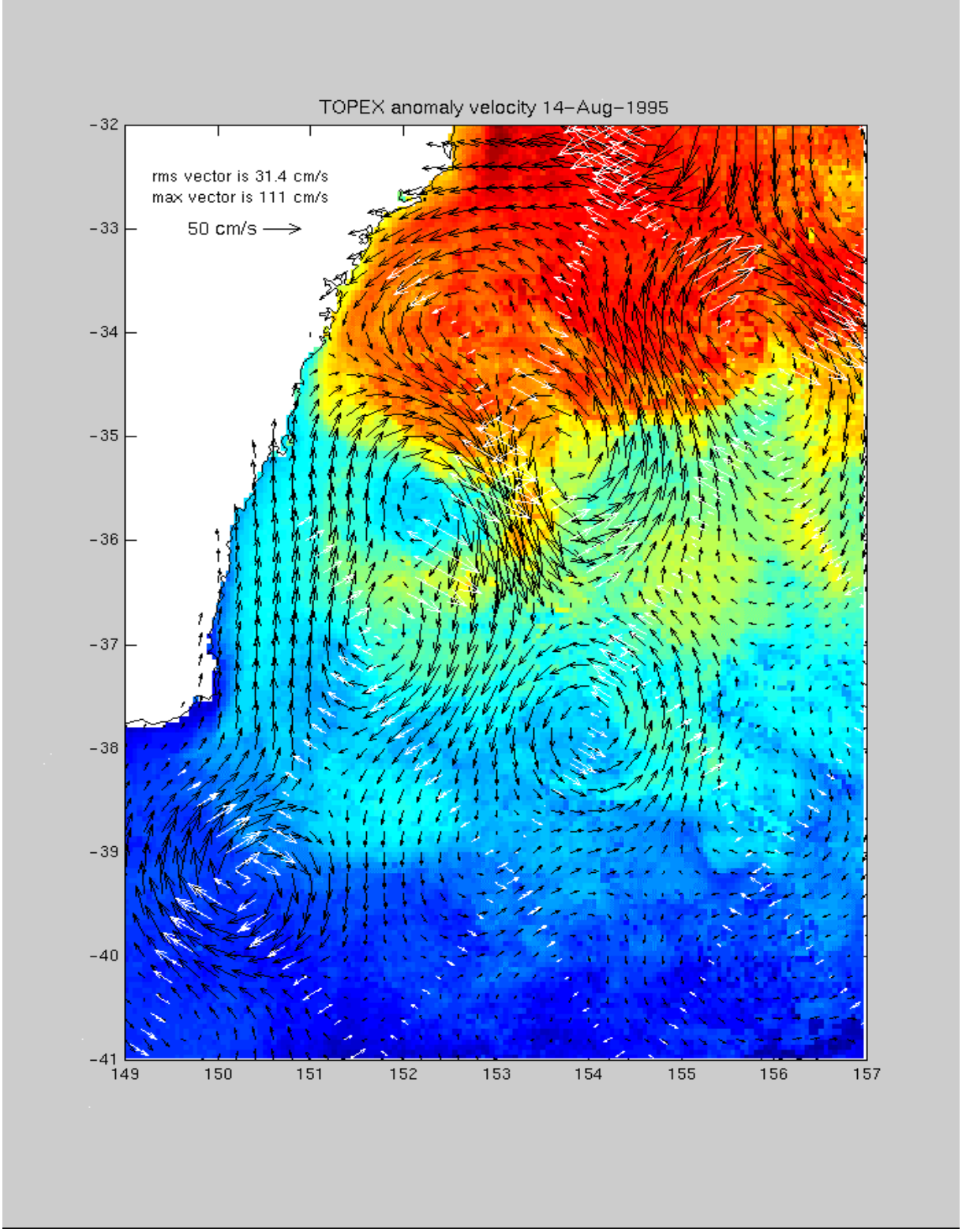

Figure 12. Southeastern coast of Australia. Black vectors – TOPEX anomaly velocity, white vectors – geostrophic currents perpendicular to the ground tracks.

Figures 13 and 14 were produced at FURG University (Fundacao Universidade do Rio Grande)– Physical Oceanography Lab (Domingues ,1999). These images illustrate how well the MCC surface vectors follow the sea surface temperature fields.

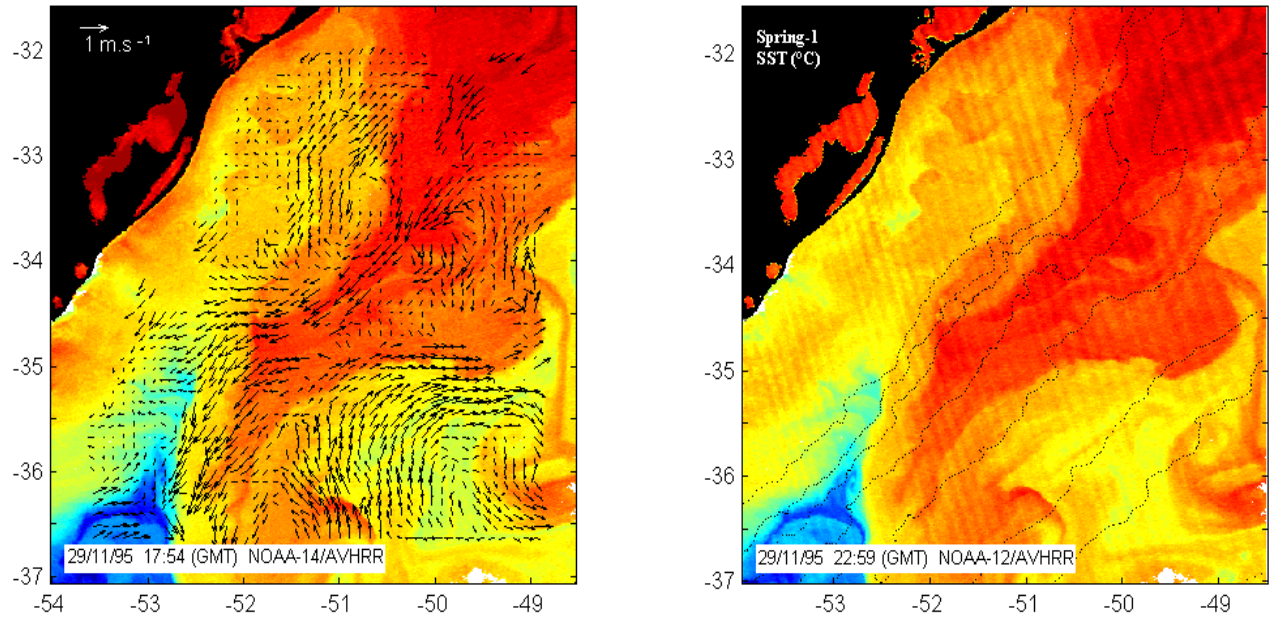

Figure 13. SST imagery of La Plata River, South America. MCC current velocity vectors overlaid.

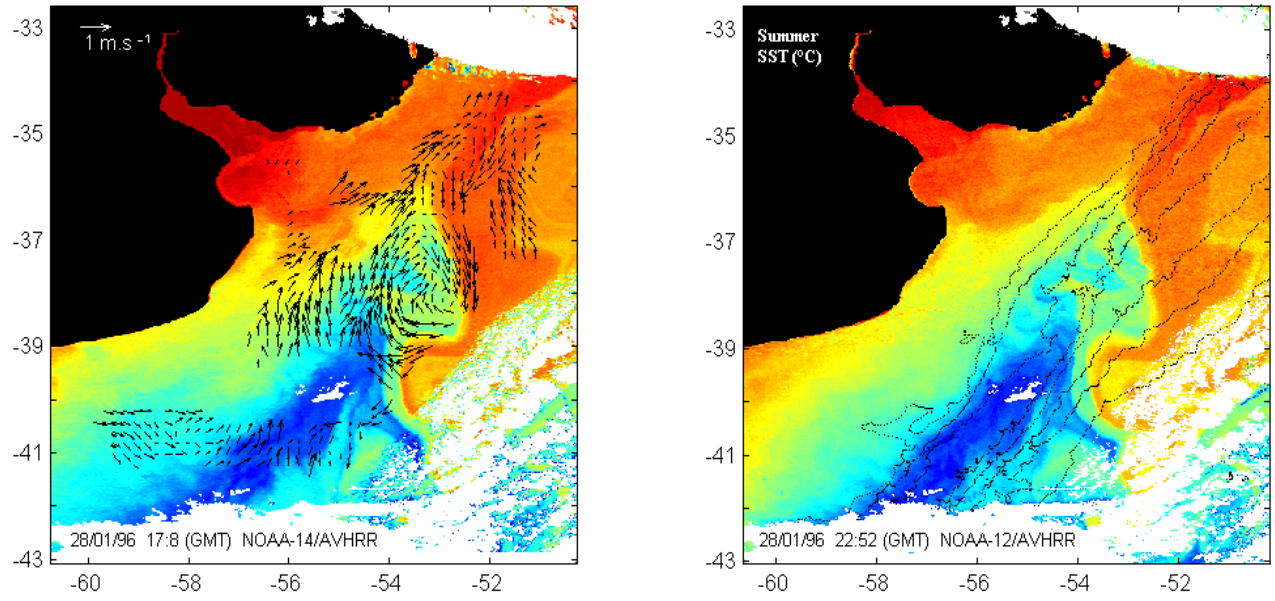

Figure 14: SST imagery of La Plata River, South America. MCC current velocity vectors overlaid.

The following figures (Figures 15-17) show the comparison between TOPEX surface height measurements to MCC surface current vectors. The inlaid altimetry data is for a ten day period. It represents the sea surface height from TOPEX/Poseidon. The larger image illustrates the ten day composite sea surface currents computed from the MCC method applied to successive sea surface temperature images. Clearly, it can be seen that the inferred MCC velocities correspond quite well to the geostrophic currents derived from sea surface heights from TOPEX.

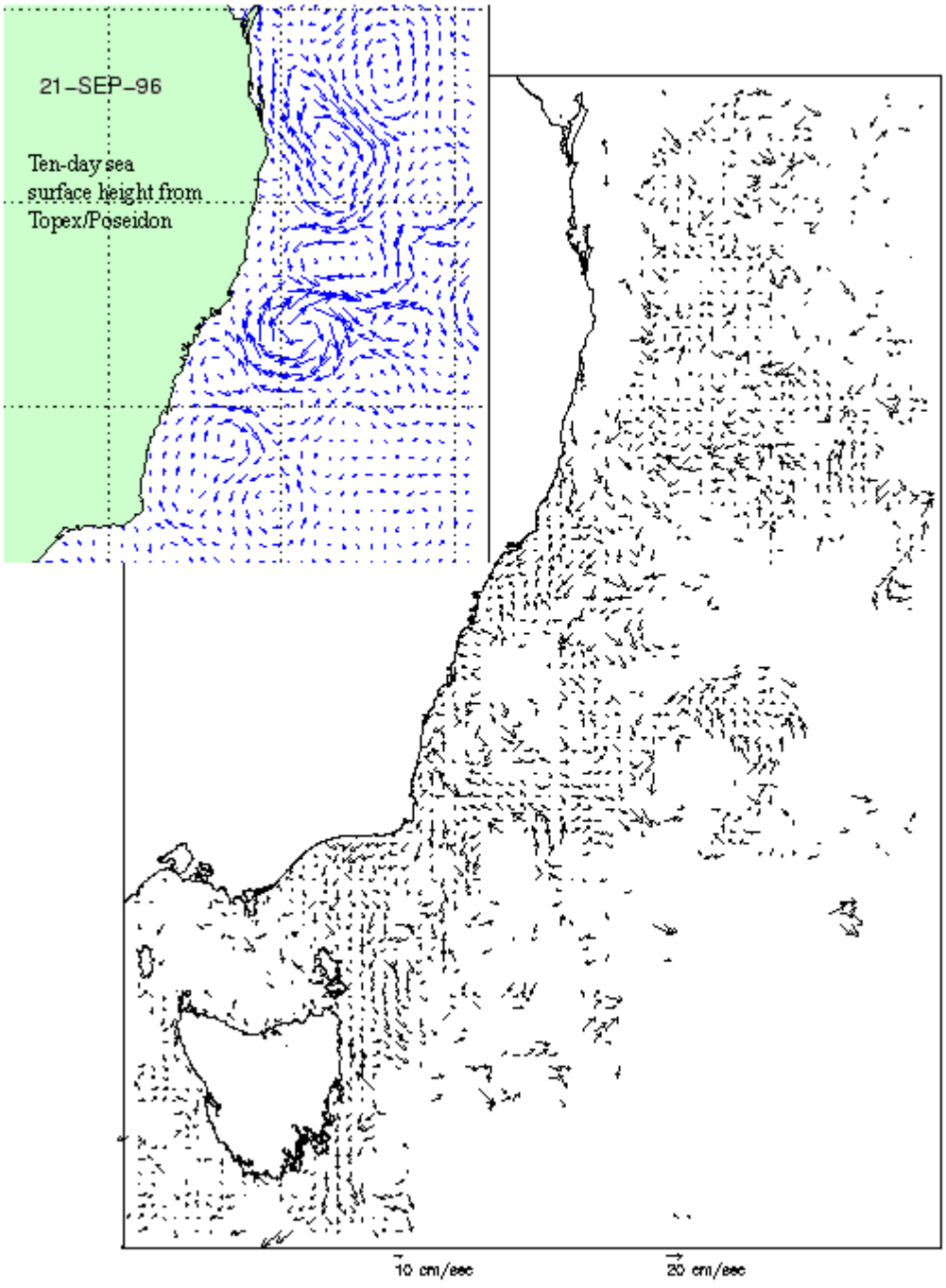

Figure 15. Ten-day composite of MCC current velocities with inlay of ten-day sea surface height from TOPEX/Poseidon. 21 Sept 96

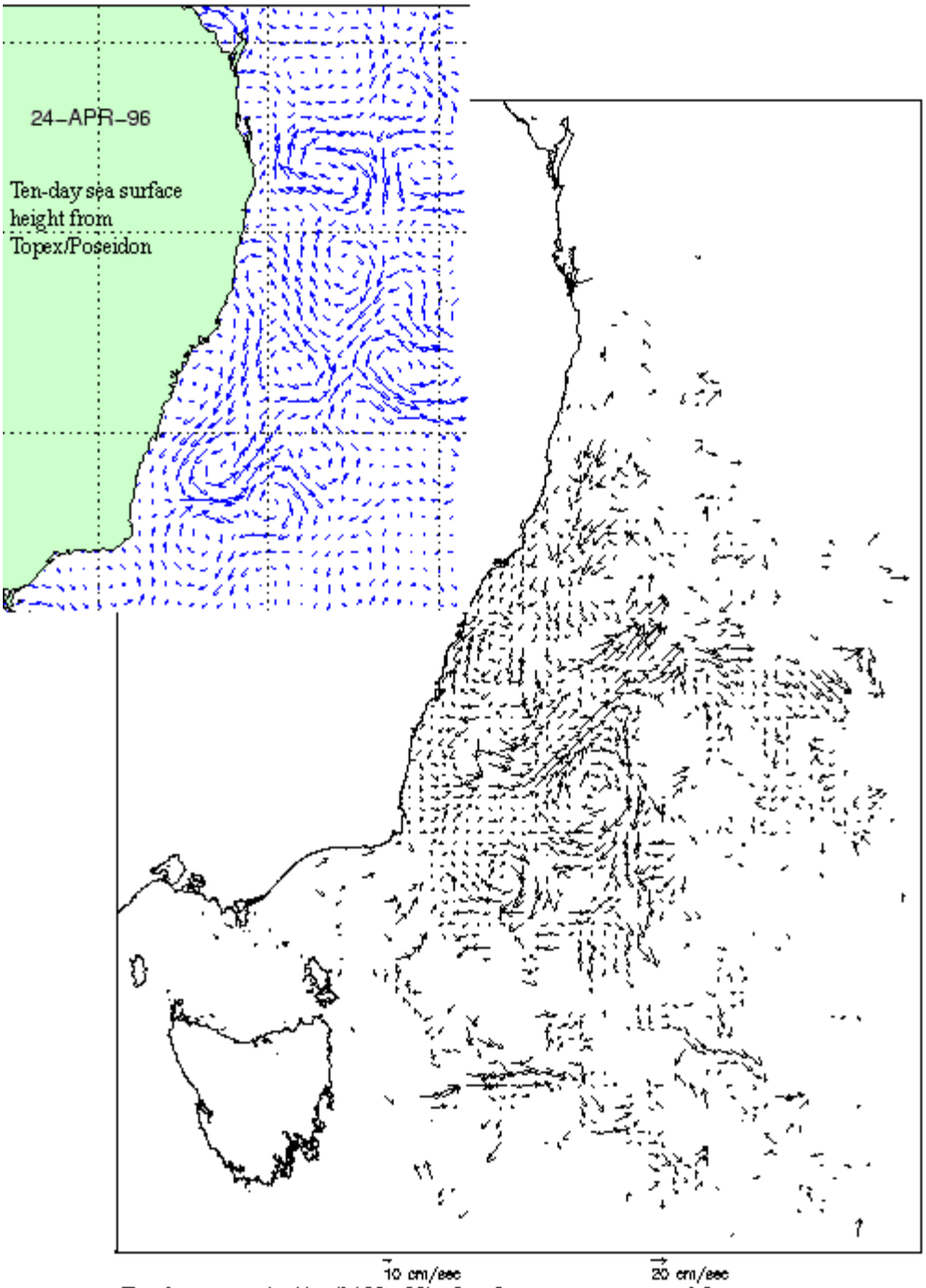

Ten-day composite (April 199 - 28) of surface currents computed from the correlations between two successive sea surface temperature images.

Figure 16. Ten-day composite of MCC current velocities with inlay of ten-day sea surface height from TOPEX/Poseidon. 24 Apr 96

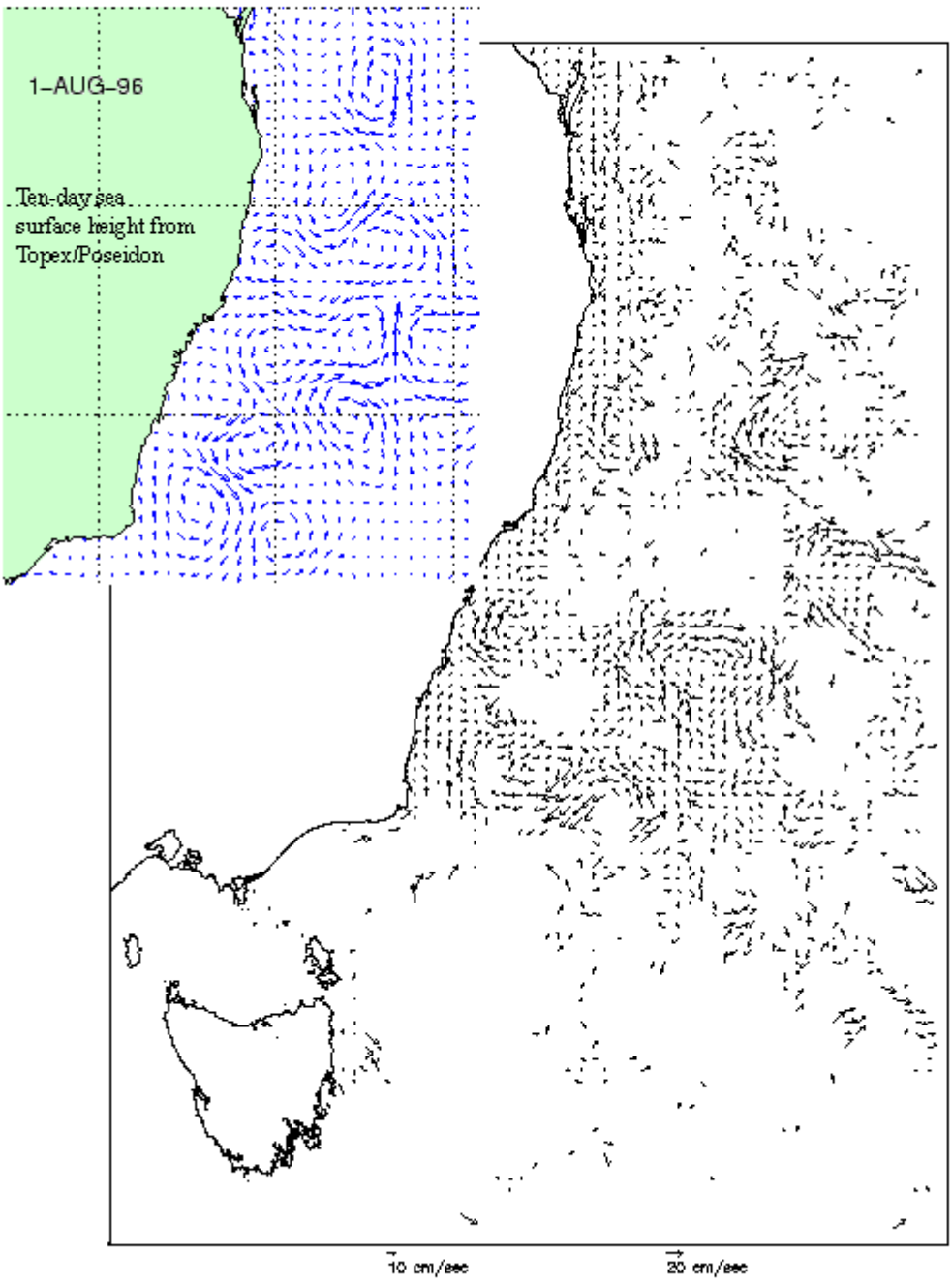

Figure 17. Ten-day composite of MCC current velocities with inlay of ten-day sea surface height from TOPEX/Poseidon. 1 Aug 96

3.4.1 Calibration Errors

Please refer to *[V-2]* and *[V-24]*.

3.4.2 Instrument Noise

The ocean current EDR is not a sensor driver for this instrument parameter. For the signal to noise sensitivity study, seven different sensor noise models supplied by SBRS were used (Hucks, 1998). The maximum cross-correlation was generated for a set of successive AVHRR SST imagery by using the MCC (maximum cross-correlation) method.

3.5 PRACTICAL CONSIDERATIONS

3.5.1 Numerical Computation Considerations

The MCC method is not Central Processing Unit (CPU)-intensive. It is an I/O program in which a lot of information is being processed as the template and search window move throughout the entire image.

3.5.2 Programming and Procedural Considerations

The MCC method is not CPU-intensive, and no ancillary data is needed to compute the current velocities. More computational time is required to process the global data set. However, this most likely is comparatively quick relative to the other EDRs.

3.5.3 Configuration of Retrievals

Please refer to *[V-2]* and *[V-24]*.

3.5.4 Quality Assessment and Diagnostics

A number of parameters will be reported in the Ocean Current product as retrieval diagnostics. These could include the MCC value for each pixel, the statement addressing whether the data is ocean color or SST, and statistical information about the processing. Summaries of these parameters will be reviewed for quality assessment by the VIIRS team. Quality assessment also could be made on the basis of the buoys deployed and the CTD surveys conducted.

3.5.5 Exception Handling

Ocean surface current velocities are calculated only if valid SST and/or ocean color retrieval values exist for the region being processed.

Only imagery that has a temporal interval between 4 and 23 hours should be utilized to compute the sea surface velocities. In a study of the Gulf Stream, Emery *et al.* (1992) showed that velocities computed by the MCC method from imagery separated by more than 24 hours were not reliable.

Clouds block out both the infrared and visible wavelengths, making it impossible to discern the SST and ocean color surface patterns. Because of this, there is a major problem in calculating

and mapping the sea surface currents from sequential imagery. Thus, it becomes imperative that clouds within the satellite imagery be identified and masked in order for the imagery to be utilized at all. Regions that are not cloud covered will have the MCC velocity vectors determined. Clearly, other regions will not have any values.

It must be considered whether there is great merit in calculating the coastal ocean current velocities. Frequently, areas of interest are continuously cloud-covered, so that rendering a velocity value becomes impossible. This would have a great impact on real-time military operations as well as on scientific research.

Please refer to *[V-2]* and *[V-24]*.

3.6 ALGORITHM VALIDATION

In situ oceanographic data are required for validation of this algorithm. Calibration on a small scale would be easy because only a few sites would be needed. The global calibration is much more difficult, but can be made with ships of opportunity; current meters, CTD surveys, and buoys.

The first issue to address is the disparity between the MCC currents and those measured by any other conventional means. As stated above, the MCC currents are a combination of all of the current types present at a specific location. This includes the tidal currents, wind driven currents, wind driven transients, and geostrophic currents (both baroclinic and barotropic). Also, the various current measurement methods vary greatly. Drifting buoys often have an uncertain coupling to the water. The more recently developed deep float systems are even less clear in defining the currents in which they flow. They are measuring some superposition of currents. Current meters moored at a specific depth resolve that depth, but not other depths. These also are subject to limitations imposed by the sensor type and its electronics. Now that the sensors range from mechanical, electrical, and acoustical, the currents resolved by these methods are even less clearly defined. Clearly, the dynamic heights methods along with satellite altimetry can only give us the geostrophic currents.

Satellite altimetry measures the surface geostrophic current provides global coverage on a multi-day repeat (at present, 10 days). One advantage of the altimeter coverage is that for a small area the data cover only a few days and are more "synoptic" than similar geostrophic currents computed from ship survey data. The MCC currents represent some superposition of all of the types of currents contributing to the ocean surface current while the satellite altimetry are only geostrophic surface currents. The degree to which the surface current is dominated by the geostrophic component is a function of location and time.

Since the primary method of surface current computation will be the maximum cross correlation (MCC) between sequential images, the challenge of validating these current estimates requires an independent set of *in situ* surface current measurements.

The best surface current measurements for this comparison are those made by Lagrangian drifting buoys that report by satellite using the ARGOS system on the NOAA polar orbiters. Surface drifters measure the current where drogued. It is important to not drogue too shallow or the drifters become involved with the surface wave field which collapses the drogue. Generally,

a 15 m depth is used for surface current drogue position. One advantage to this approach is that the data are telemetered via the ARGOS satellite system so you have the data in near real-time for your validation study.

Once deployed these buoys operate autonomously giving position and 32 words of additional data such as atmospheric pressure, and sea surface temperature. These buoys have evolved in the past couple of decades and they are now much better Lagrangian followers providing an excellent source of surface current data. As far as accuracy is concerned, it is believed that the buoys are positioned with about 0.5 - 1.5 km accuracy. Assuming about a day between positions, this gives one a current speed accuracy of about 0.017 cm/s. So, the accuracy of the positioning is more than adequate for our calibration purposes.

Another source of *in situ* information would be the geostrophic currents computed from standard oceanographic surveys. Unlike the buoys, these are very manpower-intensive and can only be done at specific times and locations. Similarly, current meters should not be moored too close to the surface in order to avoid surface wave influence. There are current meters that are influenced less by the wave field. An example of this is the vector-measuring current meter that uses orthogonal propellers and not rotors. Aanderra has developed a special rotor that is influenced less by wave action. Also, these moorings are expensive and require considerable maintenance. At the same time, there are an increasing number of surface float deep-sea moorings being established on a "permanent" basis. These moorings could be used for a near-surface current meter that would telemeter the data in near real-time.

Finally, moored current meters can provide spatially limited sampling of near surface currents. The current meters will measure more than the geostrophic current. Thus, each type of current measuring device must be used where appropriate. The geostrophic flow is best used in conjunction with satellite altimetry that allows for a lot of surface mapping.

Coastal Radar (CODAR) is a line of sight system that looks directly at the ocean surface. It is best for a monitoring application where it is important to continuously monitor the surface currents. These systems cannot measure very far out from the coast but can be used to monitor the surface current vectors continuously in the local area. The coastal direct beam radar can be used to compute fairly dense spatial arrays of surface currents in specific areas. These are particularly useful in coastal regions where there is a great need to define clearly the spatial pattern of coastal currents. CODAR measures surface currents by surface backscatter. These systems are accurate to about 2-4 cm/s and about 10 degrees in direction. Again, they are only useful for a relatively small coastal region that needs constant mapping. It must be noted that CODAR is largely uncalibrated. Thus, until that is rectified it would be difficult to use CODAR data as validation data for the MCC.

It is important to realize that the MCC method will not function in all regions and all times/seasons. Thus, it will be necessary to collect a lot of surface velocity information to validate the MCC method. It should also be emphasized that both the SST and the ocean color can be used to compute the MCC currents and so only regions where there are no gradients in SST or ocean color will be a problem.

Validation Data

Two different types of validation data are proposed. First, a number of drifting buoys that will continually provide surface current information over a few years should be deployed. It should be noted that these buoys will measure both SST and Lagrangian motion. Thus, they will validate a primary EDR, SST. These should be deployed both in regions where the MCC method will be fairly successful and in areas where the success of the method is less confident. At least 50 buoys worldwide are required. The buoys cost about two thousand each and the ARGOS costs add about that much again and maybe a bit more if they have a long service life. These buoys would all be drogued at the 15-m depth. This seems to be effective in reflecting the surface currents. Also, a 15-m drogue was used in all the World Ocean Circulation Experiment (WOCE) buoys that have provided a historical data set for comparisons with our newly collected trajectories.

A second type of validation would be concentrated surveys where a research ship is needed to collect a variety of relevant information. First, a few moorings with near-surface current meters should be deployed. To avoid the problems of the near surface wave field, the vector measuring current meters or electromagnetic current meters must be used. A minimum of 3 and a maximum of 5 moorings would be best. They should be separated widely to be able to provide boundary values for a fairly large area. Over this same area, the ship should collect traditional hydrographic data of temperature and salinity profiles. These data can be used to compute geostrophic currents that can be compared to the coincident MCC surface currents. There should be between two and ten surveys. Surveys should be performed in regions where the MCC currents will work well and in regions where the method will have some problems.

The cost of ship time is approximately $10-20 thousand per day for most ships. The infrastructure—winches as an example—is needed to do the work described above. The addition of this equipment would increase the survey costs. To minimize the cost of the validation program to the NPOESS program, a collaboration with the ocean science community in order to take advantage of projects that would produce data for use in the validation of VIIRS. This assumes that validation is not a one-time exercise, but rather a program that will provide continuous data to reference the VIIRS against. The strongest candidate data sets for such a validation program are surface float moorings that can be instrumented with near-surface current meters, ships of opportunity that could deploy drifting buoys, CODAR to measure surface currents and satellite altimetry to measure geostrophic currents.

Another approach would be to pick a certain area that has both good MCC currents and some that are more unpredictable. The measurements in this small region could be extrapolated out to other regions. This would certainly cost less, but one would never know if the collected data characteristic of the regions sampled with the MCC method are truly coincident with the other regions.

It must be realized that relatively weak currents that are difficult to resolve with most measurement techniques dominate much of the open ocean. These will not be easy to map with the MCC method and will be just as difficult to validate with related *in situ* measurement efforts. The currents of real interest are in the broader coastal areas, western boundary current regions, Antarctic Circumpolar Current and other such areas known to be dominated by relatively strong currents (say > 5-10 cm/s). Thus, one should design a validation plan to optimally measure these

stronger surface currents. This plan should take advantage of unrelated ocean research program that will collect data that are useful to this validation plan. It should also work with the ocean research community in establishing ocean monitoring programs that can provide continued measurements for the ongoing validation of VIIRS data products. It is not enough to validate/calibrate the VIIRS data once early after launch but it is necessary to have access to accurate validation data throughout the life of the VIIRS instrument. The best validation for ocean currents will be satellite altimetry and ship of opportunity programs (XBT, drifting buoy launching).

In concentrating on coastal regions, western boundary currents and other strong ocean currents the validation plan will consist of both VIIRS deployed components and other useful data deployed for other ocean research projects. There will be an emphasis on real-time data delivery to make the routine ongoing assessment of VIIRS data possible. The first step is to identify the regions where surface current measurements are needed. A suggestion would be Gulf Stream region south of Cape Hatteras, Atlantic North Equatorial Current, Canary Current and Azores Current. The two options for these measurement sites are moored current meters and repeat deployment of drifting buoys. Buoys would be reseeded at a rate to keep at least one buoy in the main area of the current at a particular time. Thus, the Gulf Stream Current would require a new buoy every few months while the eastern boundary current region may need only 1 or 2 buoys per year. All of these buoys should be drogued at 10-15 m depth to avoid the surface wave field.

There are a number of permanent moored buoy installations being proposed and it should be possible to work with these groups to add near surface current meters that would be reported in near real-time. All of the proposed buoys have surface floats and will be reporting in real-time all of the measurements collected. It is recommended that an evaluation be made of the present current meters and their ability to perform in the near surface wave field.

Other important areas include the northern gyre in the Pacific, Antarctic Circumpolar Current, Brazil Current, Benguela Current, East Australian Current, Agulhas Current, Somalia Current and the Monsoon Current. Not all of these need to be studied at the same time. A phased approach is the best first concentrating on well-known regions such at the North Atlantic or the North Pacific. Many aspects of the VIIRS validation will not be regionally dependent and any one of these basins should be able to provide measurements to assess the overall performance of the sensor.

The calibration plan may call for measurements that would provide assessment of other observations that can then be used as a secondary standard against which to evaluate the MCC currents. For example, *in situ* CTD casts might be compared with coincident TOPEX/Poseidon altimeter data in terms of dynamic height to evaluate the accuracy of the TP altimetry. Subsequently, the altimeter data could be used as the measurement standard for the evaluation of the of the MCC currents. So, coincident CTD hydrographic profiles can be evaluated in terms of the computed dynamic height and compared with the MCC profiles to determine just how these two very different sampled parts of the geostrophic current are the same. This comparison may make it possible to take advantage of the high temporal and spatial coverage of the satellite altimeter when compared with the mean field CTD density profile data.

4.0 ASSUMPTIONS AND LIMITATIONS

4.1 ASSUMPTIONS

The MCC method is used under certain assumptions. The three basic assumptions are that: The motion is horizontally advective everywhere; there is no vertical motion; and there is no heating/ cooling for SST imagery. The horizontal advection assumption holds only if the interval between successive imagery is less than 24 hours. Heating and cooling can hinder the use of SST for mapping the surface currents, while biological activity and chemical dissolution can affect the ocean color imagery products. The SST retrievals are performed under clear sky conditions only. The sea surface temperature values generated represent skin surface temperatures. In that regard, it is not reasonable to assume that the velocities of the first 5 meters of the water column correspond to the surface velocities. Ocean color algorithms would allow retrieval values to be obtained to a depth of possibly one-meter. The use of ocean color would be important in regions where the SST has no gradient, as in the tropics and the subtropics. In these regions, the ocean color displays strong gradients. Presently, it is impossible to get current velocities at these depths with an optical sensor alone. Thus, it would be beneficial to develop an algorithm to incorporate the ocean color and SST measurements for the upper layer of the coastal ocean.

4.2 LIMITATIONS

Clouds exist in the imagery. Therefore, cloud filtering must be undertaken and the clouds must me masked. Cloud cover makes it difficult to map the entire image of surface currents at the same time because they block out the infrared and visible portions of the spectrum. Thus, changes in the ocean color and SST patterns cannot be detected for the cloud covered regions. However, the cloudy regions are identified and the ocean surface currents are determined for the cloud-free regions of the image pair.

The algorithm does not explicitly solve for rotation and deformation. However, Emery *et al.* (1992) determined that if the search window is increased in size, then the rotational motion can be resolved sufficiently.

5.0 REFERENCES

Barrick, D.E., M.W. Evans and B. Weber, 1977,Ocean surface currents mapped by radar, *Science,*vol. 198, pp. 138-144.

Domingues, C.M. G.A. Goncalves, R.D. Ghisolfi and C.A.E. Garcia, 1999, Advective surface feclosities derived from sequential infrared images in the southwestern atlantic ocean, submitted to *J. Rem. Sens. Envi.*

Emery, W.J., A.C. Thomas, M.J. Collins, W.R. Crawford, and D.L. Mackas (1986). An objective procedure to compute advection from sequential infrared satellite images. *J. Geophys. Res.,* 91, 12865–12879.

Emery, W.J., C.W. Fowler, J. Hawkins, and R.H. Preller (1991). Fram Strait satellite image derived ice motions. *J. Geophys. Res.*, 96, 4751–4768.

Emery, W.J., C.W. Fowler, and C.A. Clayson (1992). Satellite image derived Gulf Stream currents, *J. Oceanic and Atm. Sci. Tech.,* 9, 285–304.

Emery, W.J. (1998). Mapping and monitoring global sea surface currents (GLOSSC), submitted *J. Oceanic and Atm. Sci. Tech.*

Emery, W.J., C. Rathbone, and P. Tildesley (1998). Combining surface currents computed from sea surface temperature and ocean color satellite imagery, submitted *J. Oceanic and Atm. Sci. Tech.*

Emery, W.J. 1999, personal communication

Fowler, C. (1995). Ice motion derived from satellite remote sensing with application to ice studies in the Beaufort sea. Dept of Aerospace Engineering Sciences, University of Colorado, Dissertation, 97 pp.

Garcia, C.A.E., and I.S. Robinson (1989). Sea surface velocities in shallow seas extracted from sequential coastal zone color scanner satellite data, *J. Geophys. Res.,* 94, 12681-12691.

Harlan,J.A., T.M. Georges, and D.C. Biggs, 1998, Comparison of over-the-horizon radar surface-current measurements in the Gulf of Mexico with simultaneous sea truth, vol. 33 (4), pp. 1241-1247.

Hucks, J. (1998). RSTX internal memo Y1629.

Kamachi, M. (1989). Advective surface velocities derived from sequential images for rotational flow field: Limitations and applications of maximum cross correlation method with rotational registration. *J. Geophys. Res.,* 94, 18,227 – 18,233.

Kelly, K.A., and P.T. Strub (1992). Comparison of velocity estimates from advanced very high resolution radiometer in the coastal transition zone, *J. Geophys. Res.,* 97, 9,653-9,668.

Maury, M. F. (1874). *The Physical Geography of the Sea*. Nelson, New York.

Ninnis, R.N., W.J. Emery, and M.J. Collins (1986). Automated extraction of sea ice motion from AVHRR imagery. *J. Geophys. Res.,* 91, 10725–10734.

Richardson, P. L. (1982). Gulf Stream rings. In "Eddies in Marine Science" (A.R. Robinson, ed.), Springe-Verlag, New York.

Rosborough, G.R., D. Baldwin, and W.J. Emery (1994). Precise AVHRR image navigation. *IEEE Geosci. Rem. Sens. IEEE GRS,* 32, 644–657.

Schott, G. Geographie des Atlantischen Ozeans, 3rd ed., C. Boysen, Hamburg, Germany, 1942.

Svejkovsky, J. (1988). Sea Surface flow estimation from advanced very high resolution radiometer and the coastal zone color scanner: a verification study. *J. Geophys. Res*., 93, 6735-6743.

Sverdrup H. V., M.W. Johnson and R. H. Fleming (1941). *The Oceans: Their Physics, Chemistry and General Biology.* Prentice-Hall, New Jersey.

Tomakian, R.T., P.T. Strub, and J. McClean-Padman (1990). Evaluation of the maximum cross-correlation method of estimating sea surface velocities from sequential satellite images. *J. Atmos. Oceanic. Tech.,* 7, 852–865.

Wu, Q. X., D. Pairman, S. J. McNeill and E.J. Barnes (1992). Computing Advective Velocity from satellite images of SST. *IEEE Trans. Geosci. Rem. Sens,* 30, 166-175.

Wyrtki, K. and G. Meyers (1976). The trade-wind field over the Pacific Ocean. *J. Appl. Meteorol.* 15, 698-704.